Norwegian University
of Life Sciences

Master's Thesis 2016 60 ECTS
Department of Chemistry, Biotechnology and Food Science

Dynamics of PML Bodies During Epidermal Cell Division in Mice

Ingrid Olstad
Master in Biotechnology

Acknowledgements

This study marks the closure of five years of studies in Biotechnology at the Norwegian University of Life Sciences (NMBU), Department of Chemistry, Biotechnology and Food Science (IKBM). The experimental part of this thesis have been performed in the Experimental Cancer Therapy research group at the Department of Medical Biochemistry (MBK), Oslo University Hospital, with Stig Ove Bøe Ph.D. (group leader), Anna Połeć Ph.D. M.Sc. (postdoc) and Professor Dzung Bao Diep as supervisors. The project was performed during fall 2015 and spring 2016 and was financed by Helse Sør-Øst.

I would like to express my gratitude to my supervisors Anna, Stig Ove and Dzung for great supervision during this thesis. Anna, thank you for always answering my questions and help with performing the experiments. Thank you Stig Ove for helpful guidance and being encouraging, and to Dzung for your interest in this project and for technical guidance.

I would also like to thank colleagues in the Experimental Cancer Therapy research group and at MBK for the supportive work environment and interesting scientific discussions. This have been a great year.

Several people have contributed to make this thesis possible. I owe my sincere thanks to Catherine Jackson for generously providing the protocol for isolation and cultivation of mouse epidermal keratinocytes. I am also grateful to Xianwen Chen Ph.D. at the Norwegian Institute for Nature Research and Alexander D. Rowe Ph.D. for help with the statistics regarding the orientation of the cell divisions and the distribution of promyelocytic leukemia in daughter cells.

Finally, I would like to thank my family, friends and my boyfriend Martin for your endless support, curious questions and all the fun we have.

Oslo, May 13 2016

Ingrid Olstad

Abstract

The tumor suppressor protein promyelocytic leukemia (PML) is the most common fusion partner to the retinoic acid receptor alpha (RARA) in acute promyelocytic leukemia (APL) patients. The two therapeutic drugs arsenic trioxide (ATO) and all-*trans* retinoic acid (ATRA) attacks the PML and RARA moiety of the oncoprotein PML-RARA, respectively, causing clinical remission. The molecular mechanisms behind these clinical treatments are of great interest as they may also contribute to treatment of other cancers.

This thesis analyses the behavior of the PML protein both *in vivo* and *in vitro* by sectioning mice embryos and by culturing mouse epidermal keratinocytes (MEKs) and mouse epidermal fibroblasts (MEFs) isolated from skin. A unique property of this protein is that it forms nuclear structures called PML bodies. Mitotic cells were identified in the basal layer of mouse epidermis and in cultured MEKs and MEFs before PML bodies were quantified in each daughter cell. PML bodies were found to become distributed symmetrically between daughter cells. This result, contrasts recent research in human cultured keratinocytes where complete asymmetric distribution of mitotic PML bodies occurs in more than 25% of dividing epidermal keratinocytes. Therefore, different mechanisms of distribution of PML bodies during mitosis might be used in mice and human cells. The angle of the mitotic axis was further analyzed in both PML wildtype and PML depleted mice. We found that the PML depleted mice tends to have a more random orientation of the cell division axis. This randomization might affect growth of the epidermis leading to a delayed or altered development compared to wildtype mice of the same developmental stage. PML bodies were also found to aggregate in mitotic MEKs, and to co-localize with nucleoporins after mitosis to generate cytoplasmic assemblies of PML and nucleoporins (CyPNs) after ATO-treatment.

These findings illustrate that PML bodies in mouse epidermis utilizes some of the same mechanisms as in human cells, including the ability to aggregate during mitosis and to form CyPNs in the presence of ATO. However, as PML bodies become symmetrically distributed in mitotic basal cells in mice, asymmetric partitioning of PML bodies does not appear to contribute to downregulate the protein levels in suprabasal layers. Differences such as these are valuable to consider when utilizing mice as a model organism when studying different aspects of APL.

Sammendrag

Tumor-suppressor proteinet promyelosytisk leukemi (PML) er det mest vanlige fusjonsproteinet til retinsyre-reseptor alfa (RARA) i akutt promyelosytisk leukemi (APL) pasienter. Medikamentene arsenikk trioksid (ATO) og all-trans retinsyre (ATRA) angriper hver sin del av onkoproteinet PML-RARA med klinisk remisjon som følge. Det er stor interesse for de molekylære mekanismene bak behandlingen av APL med mulighet for at liknende terapeutiske mekanismer kan bidra til behandling av andre kreftformer.

Denne masteroppgaven analyserer PML-proteinets adferd både *in vivo* og *in vitro* ved snitting av museembryo og dyrkning av keratinocytter (MEKs) og fibroblaster (MEFs) fra mus isolert fra hud. En unik egenskap ved proteinet er at det danner nukleære strukturer kalt PML bodies. Mitotiske celler ble identifisert i basallaget i epidermis og i dyrkede MEKs og MEFs før PML bodies ble kvantifisert i hver av dattercellene. Vi fant at PML bodies blir symmetrisk distribuert mellom dattercellene. Dette resultatet motstrider tidligere forskning på dyrkede humane keratinocytter hvor total asymmetrisk fordeling av PML bodies forekommer i mer enn 25% av mitotiske epidermale keratinocytter. Dermed er det mulig at forskjellige mekanismer blir brukt fra mus og menneske til å distribuere PML bodies i løpet av mitosen. Videre ble vinkelen på celledelingen analysert i både villtype og PML negative mus. Vi oppdaget at PML negative mus ser ut til å ha en mer tilfeldig orientering av celledelingsaksen. Den tilfeldige orienteringen av celledelingen i PML negative mus kan muligens påvirke vekst av epidermis og dermed føre til en forsinket eller endret utvikling sammenliknet med villtype mus av samme embryoniske alder. Vi fant også at PML bodies aggregerer i mitotiske MEKs, i tillegg til å kolokalisere med nukleoporiner etter mitosen og generere "cytoplasmic assemblies of PML and nucleoporins" (CyPNs) etter behandling med ATO.

Disse resultatene illustrerer at PML bodies i epidermis i mus benytter noen av de samme mekanismene som i humane celler, inkludert muligheten til å aggregere under mitosen og til å danne CyPNs ved tilstedeværelse av ATO. Siden PML bodies ble symmetrisk distribuert i mitotiske basalceller i mus, betyr dette at asymmetrisk fordeling av PML bodies ikke ser ut til å bidra til å nedregulere proteinnivået i suprabasale lag. Ulikheter slik som dette er verdifulle å vurdere ved bruk av musemodeller i APL-studier.

Abbreviations

AML	Acute myelogenous leukemia
aPKC	Atypical protein kinase C
APL	Acute promyelocytic leukemia
ATO	Arsenic trioxide
ATRA	All-*trans* retinoic acid
Baz	Bazooka
BSA	Bovine serum albumin
CC	Coiled-coil
Cdk	Cyclin-dependent kinase
CNS	Central nervous system
CyPNs	cytoplasmic assemblies of PML and nucleoporins
DAPI	4',6-diamidino-2-phenylindole
Daxx	Fas death domain-associated protein
DMEM	Dulbecco's Modified Eagle Medium
DMSO	Dimethyl sulfoxide
DPBS	Dulbecco's phosphate buffered saline
E	Embryonic stage
ECM	Extracellular matrix
EGF	Epidermal growth factor
FBS	Fetal bovine serum
FOTS	Forsøksdyrforvaltningens tilsyns- og søknadssystem
GMC	Ganglion mother cell
GS	Goat serum
HaCaT	Cultured human keratinocyte
HCl	Hydrogen chloride
HDF	Human dermal fibroblast
HSC	Hematopoietic stem cell
IF	Immunofluorescence
IHC	Immunohistochemistry
Insc	Inscuteable
K	Keratin
Lgl	Lethal (2) giant larvae
MAPPs	Mitotic assemblies of PML proteins
MEF	Mouse epidermal fibroblast
MEK	Mouse epidermal keratinocyte
MEM	Non-Essential Amino Acids Solution
MilliQ	MQ
mInsc	Mammalian inscuteable
Mud	Mushroom body defect
NaCl	Sodium chloride
NLS	Nuclear localization signal
NPC	Nuclear pore complex

NPM	Nucleophosmin
NuMa	Nuclear-mitotic-apparatus
Nups	Nucleoporins
P	Post-natal day
Par3	Partitioning defect 3
Par6	Partitioning defect 6
PBS	Phosphate buffered saline
PCP	Planar cell polarity
Pen/Strep	Penicillin/Streptomycin
PFA	Paraformaldehyde
Pins	Partner of Inscuteable
PLZF	Promyelocytic-leukemia-zinc-finger
PML	Promyelocytic leukemia
PML NB	PML nuclear body
Pon	Partner of Numb
PPARδ-FAO	Peroxisome proliferator-activated receptor δ-fatty-acid oxidation
Pros	Prospero
RARA	Retinoic acid receptor α
RT	Room temperature
Sara	Smad Anchor for Receptor Activation
SIM	SUMO interaction motif
SOP	sensory organ precursor
SP	Spinous cell
STAT5b	Signal transducer and activator of transcription 5b
SUMO	Small ubiquitin-like modifier
TA	Transit-amplifying
TNF	Tumor necrosis factor
TRIM	Tripartite motif

Contents

1 Introduction

1.1 Skin

The skin covers the surface of the body and represents the largest organ of the body (Hsu et al. 2014). The primary function of the skin is to act as an essential barrier, which protects the body for unwanted influences from the environment, like mechanical and chemical trauma, dehydration and against pathogenic bacteria (Forni et al. 2012; Koster & Roop 2007). Throughout life, the skin receives and transmits sensory- and communication-signals and have a large capacity of regenerating after wounding. The skin cells are involved in a homeostatic process where new cells contribute to growth, maintenance of the skin and replacement of old cells that die (Fuchs 2008). The skin can be divided into the two main layers referred to as epidermis and dermis (Candi et al. 2006; Forni et al. 2012). Epidermis constitutes the outer layers of the skin comprised of proliferating basal and differentiated suprabasal keratinocytes. The underlying dermis supports the epidermis and consists of extracellular matrix (ECM) where blood vessels and nerve endings reside among other skin components.

1.1.1 Epidermis

The epidermis is multilayered and constitutes the uppermost part of the skin. It consists of 80% keratinocytes, which represents the skin epithelial cells (Bragulla & Homberger 2009). The basal layer of the epidermis, where stem cells reside, is positioned right above the basement membrane. Stem cells are undifferentiated and have the potential both to divide and to give raise to differentiated keratinocytes (Blanpain & Fuchs 2009). Transit-amplifying (TA) cells divides a limited number of times before entering a terminal differentiation program. These cells play an important role in supporting development and maintenance of the epidermis. The ability to proliferate is lost as the cells differentiate and migrate to the layers closer to the skin surface. During differentiation, a basal cell will first migrate to the spinous layer before the migration continuous to the granular layer and thereafter to stratum corneum, also known as the cornified layer (Figure 1) (Blanpain & Fuchs 2009; Candi et al. 2005; Forni et al. 2012; Koster & Roop 2007).

A group of proteins that frequently is used to characterize the different epidermal layers is keratins. This is a large family of proteins commonly expressed in epithelial cells. Keratins are intermediate filaments that form the cytoskeleton and thus provide structural stability to a keratinocyte. Keratin filaments are composed of one acidic and one basic keratin component

that form heterodimers (Blanpain & Fuchs 2006; Bragulla & Homberger 2009). The type of keratin that constitute the intermediate filament differs between different epidermal layers (Bragulla & Homberger 2009).

The basement membrane is at the "bottom" of the epidermis and represent a thin matrix rich in ECM components such as laminin V, fibronectin and collagen IV (Fuchs 2008). It contributes to the attachment of basal cells to the basement membrane (Blanpain & Fuchs 2006). The basal layer contains stem and progenitor cells that express the structural proteins keratin 5 (K5), K14 and K15 (Blanpain & Fuchs 2006; Fuchs 1995). Spinous cells switch off the expression of K5, K14 and K15 and turn on expression of K1 and K10 while cells in the granular layer produce loricrin and the precursor profilaggrin (Candi et al. 2005; Forni et al. 2012). Filaggrin is expressed in stratum corneum, the outermost layer of the epidermis. Filaggrin packs keratinocytes into tight bundles that makes the cells collapse into flattened structures. The epithelial cells in the stratum corneum are known as corneocytes. After completed process of keratinization, they are cornified and dead (Candi et al. 2005; Forni et al. 2012). Still, the stratum corneum possess the barrier-function that keeps microbes out and fluids inside an individual (Blanpain & Fuchs 2006). The corneocytes are shed off the skin surface continuously by the process desquamation (Candi et al. 2005). Therefore, it is a constant need to replenish cells executed by the stem cells in the basal layer.

The cell turnover is relatively high in adult human epidermis, and a cell uses only four weeks to become terminally differentiated. In adult mice epidermis, however, epidermal proliferation becomes slower as the hair coat develop and acts as the primary protection (Fuchs 2008). Both cell proliferation and differentiation among other proteins and factors contribute to the development and maintenance of the different layers of the epidermis.

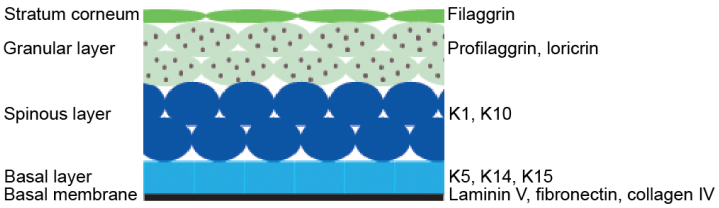

Figure 1. The different layers of matured epidermis. The epidermis consists of the layers basal membrane, basal layer, spinous layer, granular layer and the outermost stratum corneum. Each of these layers produce different factors, some of them are listed on the right side of the figure. Based on Koster and Roop (2007) and Liu et al. (2013).

1.1.2 Dermis

The dermis is the next layer of the skin and is separated from the epidermis by the basement membrane. The basement membrane is composed of components secreted from both dermis and epidermis, such as fibroblasts and ECM respectively (Blanpain & Fuchs 2006). The dermis is a thick layer of fibrous and elastic tissue, which mostly contains collagen, elastin and fibrillin. This connective tissue supports flexibility and strength of the epidermis. The dermis contains nerve endings, sweat glands, sebaceous glands and blood vessels (Blanpain & Fuchs 2009; Forni et al. 2012). Macrophages, neutrophils and lymphocytes are examples of immune cells and these can be transferred to the epidermis through the basement membrane (Forni et al. 2012).

1.1.3 Embryogenesis

An embryo develops by the process of embryogenesis. The initial stages of this process are highly conserved among invertebrates. In mammals, a fertilized egg divides and makes a hallow ball of cells named blastula (Alberts et al. 2015). Thereafter the process of gastrulation transforms the blastula into three separate embryonic layers designated gastrula, mesoderm and ectoderm (Blanpain & Fuchs 2006; Blanpain & Fuchs 2009; Forni et al. 2012). These three layers gives rise to all tissues and organs. The epidermis originates from the ectoderm and the dermis from the mesoderm (Alberts et al. 2015; Blanpain & Fuchs 2009). Subsequently, each layer of the skin will then develop into distinct functional layers.

1.1.4 Embryonic development of the epidermis in mice

During embryonic development in mice, the surface ectoderm forms at embryonic stage 8.5 (E8.5) before the basal layer assembles at E9.5 (Koster & Roop 2007). The initial stratification of the epidermis occur between E12.5 to E15.5. During this period, a protective cell layer called periderm is made concomitant with formation of the basement membrane (Blanpain & Fuchs 2006). At E14.5, an intermediate layer forms between the basal layer and periderm. However, the intermediate layer appears briefly as the intermediate cells mature into spinous cells at E15.5. In adult epidermis, there is no intermediate layer and therefore some of the cells in the basal layer migrate into the spinous layer and contributes to push cells outwards to the skin surface (Koster & Roop 2007). Cells from the spinous layer continuous the stratification and develop the granular layer at E16.5. At E18.5, the periderm sheds off and stratum corneum becomes the outermost layer of the epidermis (Figure 2). Hair follicles are one of the skin appendages. Signals from the epidermis and dermis combine to initiate the formation of hair

follicle placodes starting from E14.5 (Liu et al. 2013). Further signaling triggers the hair placode to grow down into the dermis, before maturation of the hair follicle becomes completed around post-natal day 5 (P5) (Liu et al. 2013).

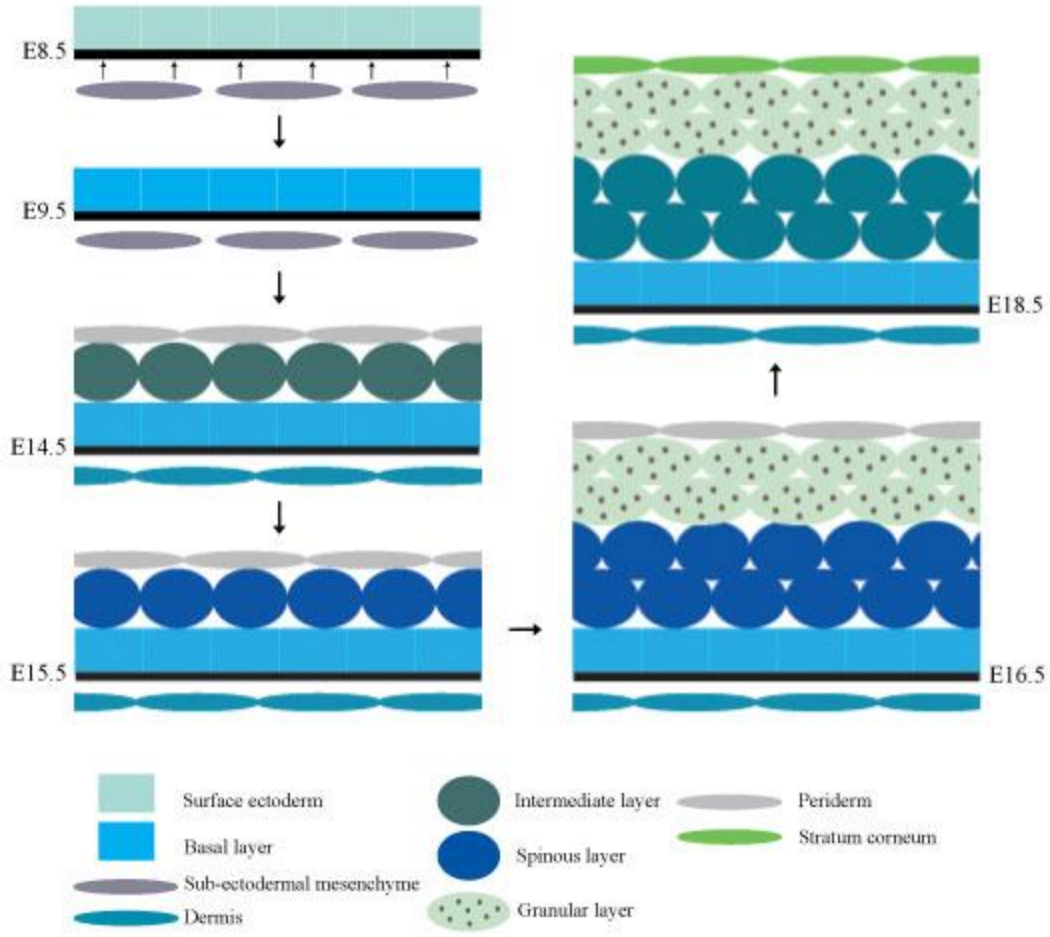

Figure 2. Development of mouse epidermis. During embryonic development from E8.5 to E18.5 the different layers of the mouse epidermis is produced. Figure based on Koster and Roop (2007) and Liu et al. (2013).

1.2 Cell division

During the lifespan of an organism, cell division occurs during tissue development, homeostasis and regeneration after wounding. This is possible as cells copy their content and divides into two new daughter cells during the cell cycle (Figure 3) (Alberts et al. 2015; Schafer 1998). The cell division cycle starts by replication of DNA in the S-phase. Thereafter a gap-phase named G_2 allows time for the cell to grow before entry into mitosis, the M-phase. The mitosis can be staged into prophase, prometaphase, metaphase, anaphase, telophase and cytokinesis. Here, the duplicated DNA, organelles, proteins and cytoplasm separate to make two new functional daughter cells. After mitosis, another gap-phase, known as G_1, is initiated that last until the cell reaches a second S-phase. Together, G_1, S and G_2 are referred to as the interphase (Schafer

1998). While cells can divide extensively during development and tissue regeneration, most cells in a tissue does not divide and enter a resting state called G_0 or quiescence (Alberts et al. 2015; Schafer 1998). The cell division cycle is highly conserved and essential for all living organisms.

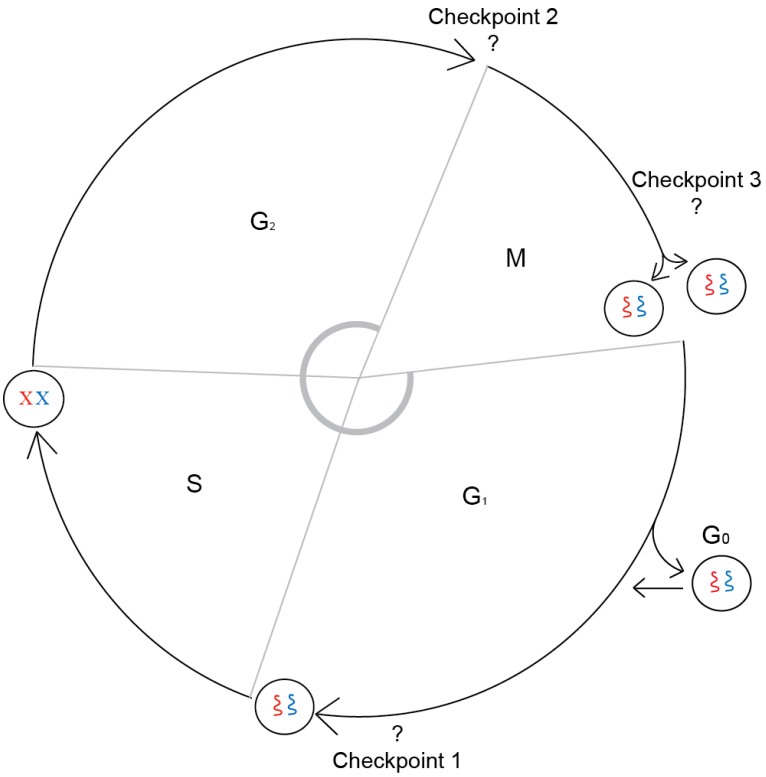

Figure 3. The cell cycle and its checkpoints. During the cell cycle, a cell will duplicate its content and subsequently divide into two daughter cells. DNA synthesis occur during S-phase and each chromosome will consist of two sister chromatids at the end of S-phase, illustrated by the two X's inside the cell. Segregation of the sister chromatids and cell division occurs in M-phase. Three checkpoints regulate progression in the cell cycle. Checkpoint 1 occurs late in G_1, checkpoint 2 is right before a cell enters mitosis and checkpoint 3 functions at the metaphase-to-anaphase transition in the M-phase. The inner grey circle represents the interphase, which consists of G_1, S-phase and G_2.

The cell cycle is tightly controlled by at least three cell cycle checkpoints (Figure 3). If there is a problem inside or outside the cell, these checkpoints block the progression of the cell cycle until the issue is fixed. Cyclin-dependent kinases (Cdks) and cyclins are key proteins that drives cell cycle progression (King & Cidlowski 1998; Schafer 1998). Cdks become activated when cyclins are bound and this complex can in turn phosphorylate other proteins that regulates cell cycle progression. Upon checkpoint activation, cdk inhibitors such as p21 are expressed leading to cell cycle arrest. p21 work together with p53 and inhibits the kinase activity of the Cdk-cyclin complexes leading to G_1 growth arrest (Abbas & Dutta 2009; Sancar et al. 2004). There are different classes of cyclins and the level of these differ during the cell cycle while the level

of Cdks are constant (Alberts et al. 2015). Some of the different Cdk-cyclin-complexes act near the checkpoints of the cell cycle (Alberts et al. 2015).

As the present thesis is more directed to the mitosis section of the cell division, the focus will be aimed at these events. During prophase, the duplicated chromosomes condensate. In this way, the chromosomes becomes compact and the separation of the sister chromatids will be more easy to complete (Alberts et al. 2015). Early in prometaphase, the nuclear membrane of a dividing cell breaks down and chromosomes becomes attached to the spindle microtubules through the protein complex kinetochores (Alberts et al. 2015; Pines & Rieder 2001). Thereafter, the mitotic spindle aligns the chromosomes near the spindle equator in metaphase before the sister chromatids are pulled apart during anaphase to their separate poles. As the mitotic spindle becomes shorter and the spindle poles move apart, these actions lead to segregation of the chromosomes. When the daughter chromosomes reaches their poles, the nuclear membrane starts to reassemble and the chromosomes decondense in telophase. In addition, the contractile ring consisting of the filaments actin and myosin starts to contract and divide the cytoplasm. Thereafter, cytokinesis completes the M-phase of the cell cycle by cleaving the cell into two daughter cells (Alberts et al. 2015; Pines & Rieder 2001).

1.2.1 Symmetric and asymmetric cell division

The terms symmetric and asymmetric cell division describes the distribution of specific cell components to the daughter cells after mitosis (Doe 1996; Horvitz & Herskowitz 1992). During symmetric division, components are distributed equally between daughter cells. In contrast, asymmetric cell division distributes components disproportionally between the daughters. Asymmetric cell division is important to generate diversity (Hawkins & Garriga 1998; Jan & Jan 1998). For example, asymmetric division of stem cells generates one daughter stem cell and one differentiating daughter cell. In this way, the pool of stem cells is maintained at the same time as different cell types differentiates and develops. This is crucial for an organism to grow, maintain a healthy homeostasis of cells and generate diversity. Asymmetric commitment of stem cells is made possible as a consequence of asymmetric partitioning of cell components known as cell-fate determinants are distributed unequally during mitosis (Jan & Jan 1998; Knoblich 2008).

1.2.2 Symmetric and asymmetric cell division in epidermis

In epidermis, the division is symmetric if both daughter cells obtain the same fate (Blanpain & Fuchs 2009). Previous studies have shown that epidermal cells divide symmetrically when both daughter cells remain in the basal layer of the epidermis. Asymmetric cell division, on the other hand, occurs if the mitotic spindle change its orientation from lateral to perpendicular in relation to the basement membrane and leads to different fates of the daughter cells (Figure 4) (Blanpain & Fuchs 2009; Liu et al. 2013). During asymmetric division, one daughter cell will remain stem cell-like in the basal layer while the other daughter cell will differentiate and migrate outwards to suprabasal layers to become terminally differentiated (Blanpain & Fuchs 2009; Fuchs 2008; Koster & Roop 2007). Asymmetric cell division can also occur when division is horizontal in relation to the basement membrane. In this case, proliferation components are distributed to the stem cell daughter and differentiating inducing components to the differentiating daughter cell. In these cases, the differentiating daughter cell must delaminate into the spinous layer (Fuchs 2008).

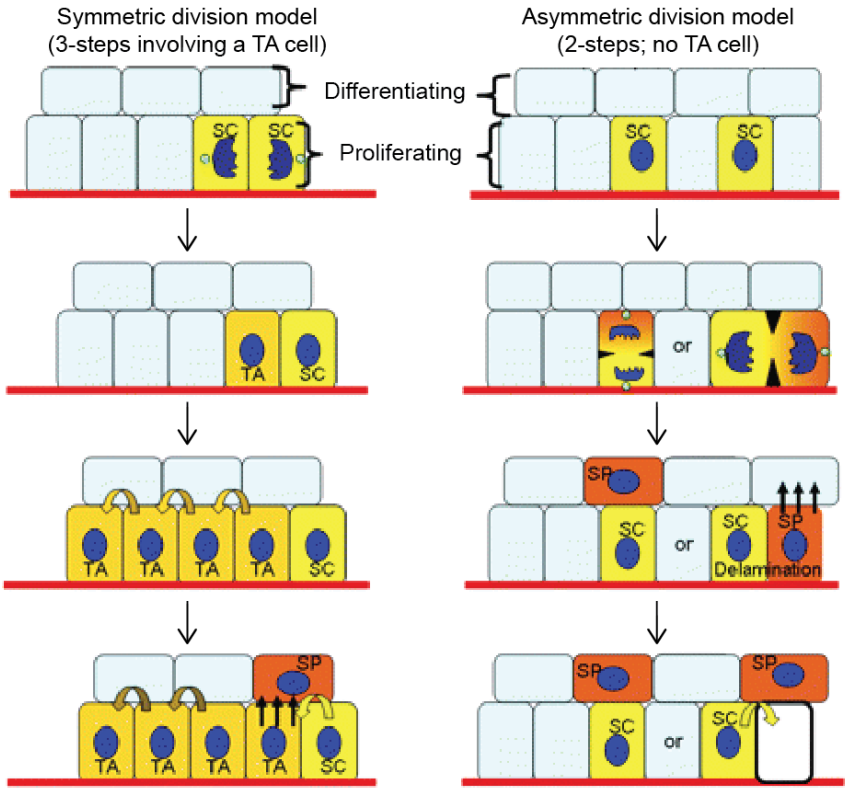

Figure 4. Symmetric and asymmetric cell division models in epidermal basal cells. In symmetric cell division, a basal cell can generate one daughter stem cell (SC) and a transit-amplifying daughter cell (TA). The TA cell can thereafter divide several times to generate new TA cells that ultimately will move upwards to become a spinous cell (SP). In asymmetric cell division, however, no TA cell is generated. The mitosis can occur horizontal in relation to the basement membrane and generate a SP cell that thereafter delaminates. The mitosis can also occur vertical in relation to the basement membrane where the SP cell automatically becomes positioned into the spinous layer. Figure adapted from Fuchs (2008).

Williams and coworkers investigated the orientation of cell division in relation to the basement membrane at different stages of wildtype mice embryos (Williams et al. 2014). During early embryonic development, the cell division was mostly planar relative to the basement membrane. From E13.5, oblique and vertical cell division started to occur. Further embryonic development had about equal amount of horizontal and vertical orientation compared to the basement membrane at E16.5 (Williams et al. 2014). This shift in orientation of the cell division reflects the growth of the basal layer during early development of the embryo before stratification and differentiation of the epidermis occur at later stages of embryonic development.

1.2.3 Mechanisms of asymmetric cell division

One of the most studied models for asymmetric cell division is neuroblasts in *Drosophila* (Knoblich 2008). The neuroblasts take part in the development of the central nervous system (CNS) where one of the daughter cells self-renew while the other develop into a ganglion mother cell (GMC), which divides once and terminally differentiate into two neurons (Doe 1992; Knoblich 2008). The mechanism behind this asymmetric cell division is reviewed in Knoblich (2008) and involves several proteins that become recruited to the cell cortex at the apical side of the cell before entering mitosis. One protein complex that accumulate at these sites is the Par complex. This complex creates cell polarity in different organisms and consists of the proteins atypical protein kinase C (aPKC), Bazooka (Baz) (partitioning defect 3 in mammals (Par3)) and partitioning defect 6 (Par6) (Betschinger & Knoblich 2004; Dewey et al. 2015; Goldstein & Macara 2007; Knoblich 2008). This accumulation of proteins induces the cell-fate determinant binding to the cell cortex on the opposite, basal side of the cell, which are subsequently inherited by the GMC. The protein Lethal (2) giant larvae (Lgl) becomes phosphorylated by aPKC and recruits cell fate determinants to the cell cortex (Betschinger et al. 2003). Phosphorylated Lgl seems to be restricted to the basal side of the mitotic cell, suggesting that this protein might contribute to the asymmetric segregation of the cell fate determinants (Knoblich 2008). The adaptor proteins Partner of Numb (Pon) and Miranda facilitate recruitment of the cell-fate determinants Numb, Prospero (Pros) and Brat to the basal cell during mitosis (Knoblich 2008; Shen, C.-P. et al. 1997). Numb inhibits Notch-mediated signaling, therefore hindering the ability of newly divided cells to self-renew and instead promotes cell differentiation of the basal cell to a GMC (Wang et al. 2006). Pros regulates transcription while the function of Brat is unknown (Knoblich 2008). The orientation of the mitotic spindle along the cell polarity axis contributes to completion of asymmetric segregation

of cell fate determinants. In *Drosophila* neuroblasts, the protein Inscuteable (Insc) localizes to the apical cortex where it binds to Par3. Thereafter, Insc interacts with the proteins $G\alpha_i$ and Partner of Inscuteable (Pins), an ortholog to mammalian LGN, which in turn recruits the protein mushroom body defect (Mud). Mud is an ortholog to mammalian nuclear-mitotic-apparatus (NuMa) (Siller et al. 2006) that interacts with dynactin and orients astral microtubules and the mitotic spindle until it aligns with the cell polarity axis (Bowman et al. 2006; Gaglio et al. 1995; Siller & Doe 2009). Together, establishment of cell polarity, segregation of cell-fate determinants and orientation of the mitotic spindle regulate the asymmetric cell division of *Drosophila* neuroblasts.

As in *Drosophila* neuroblasts, the mammalian Par complex also consists of aPKC, Par3 and Par6. In the epidermis these proteins binds to the apical cortex of mitotic basal cells generating cell polarity (Williams et al. 2014) (Figure 5). Par3 is known to interact with Insc in *Drosophila* (Knoblich 2008) and might have the same function in mammalian epidermis as Lechler and Fuchs (2005) identified the mammalian homologue mInsc. mInsc was found to bind LGN which interacts with the membrane bound $G\alpha_i$ (Williams et al. 2014). During symmetric cell division, LGN was non-polarized as it was found to be evenly distributed or absent. During asymmetric cell division, however, LGN was apically localized and might bind NuMA in a similar way as Pins binds Mud in *Drosophila* neuroblasts (Knoblich 2008; Williams et al. 2014). NuMA is known to interact with the motor protein dynactin that in turn positions astral microtubules and orient the mitotic spindle, therefore contributing to asymmetric cell division (Gaglio et al. 1995; Siller & Doe 2009). Knockdown of either *LGN* or *Numa1* in mice epidermis resulted in increased planar cell divisions during embryogenesis and supports the notion that LGN might interact with NuMA (Williams et al. 2014). As Williams et al. (2014) suggests, cell fate determinants might exist in the developing epidermis where they contribute to the asymmetric cell division. However, as far as we know, these factors have not been identified yet. Williams et al. (2014) also discovered that early stratification was not dependent on perpendicular spindle orientation and that LGN was not detected until ~E14.5 (Lechler & Fuchs 2005; Williams et al. 2014). Therefore, early stratification may be driven by delamination and later differentiation by asymmetric cell division in mice epidermis.

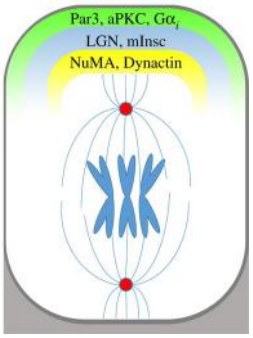

Figure 5. Molecular mechanisms orienting the mitotic spindle. During asymmetric cell division in epidermal basal cells, LGN, mInsc, NuMA and Dynactin become recruited to the apical cortex. These components orients the spindle perpendicular in relation to the basement membrane. Figure from Kulukian and Fuchs (2013).

However, not all asymmetric distributed proteins localize to the cell cortex during mitosis. For instance, Smad Anchor for Receptor Activation (Sara) endosomes, a sub-class of early endosomes (Itoh et al. 2002), have been observed to undergo asymmetric distribution in sensory organ precursor (SOP) cells in *Drosophila*. Recently, Derivery et al. (2015) described the mechanism behind the asymmetric distribution of Sara endosomes during mitosis. Late in cytokinesis, the SOP endosomes that contains Sara proteins will be distributed to the pIIa daughter cell and not to the pIIb by transportation on the central spindle located within the midbody (Derivery et al. 2015). This transportation was found to be carried out by the motor-protein Klp98A dependent on central spindle asymmetry (Derivery et al. 2015). The pIIa is the precursor for hair cells and socket cells that surrounds the base of the hair, while pIIb will develop into neuron and sheath cells along the hair shaft (Miller et al. 2009; Rhyu et al. 1994). Therefore, this asymmetric cell division SOP cells ultimately results in four different cell types.

1.3 Promyelocytic leukemia protein

The tumor suppressor protein promyelocytic leukemia (PML) is expressed in most mammalian cells (Bernardi & Pandolfi 2007; Bøe et al. 2006; Wang, Z. G. et al. 1998). PML function in several different cellular processes, including apoptosis, senescence, differentiation, genome maintenance and virus defense (Bernardi & Pandolfi 2007; Grignani et al. 1993; Salomoni et al. 2008; Wang, Z. G. et al. 1998). The gene encoding the PML protein has nine exons. Alternative splicing of exons seven to nine generate at least seven isotypes designated PML I through PML VII (Jensen et al. 2001). The N-terminus is consistent in all PML isoforms and contains a tripartite motif (TRIM). The motif is conserved in a large family of proteins (the TRIM family of proteins) and comprises a cysteine-rich zinc binding domain, RING finger domain (R) and B-boxes (B1 and/or B2), in addition to a coiled-coil (CC) region (Jensen et al.

2001; Reymond et al. 2001). Sumoylation occurs when proteins become covalently linked to the small ubiquitin-like modifier (SUMO) protein (Bernardi & Pandolfi 2007; Shen et al. 2006; Zhong et al. 2000a). The SUMO-conjugating enzyme UBC19 catalyzes the sumoylation of three lysine residues, at the amino acid positions 65, 160 and 490 respectively, leaving PML covalently bound to SUMO (Bernardi & Pandolfi 2007; Lallemand-Breitenbach 2010; Zhong et al. 2000a). This makes the sumoylated PML tightly associated to the nuclear matrix. In addition, PML contains a SUMO interaction motif (SIM), which makes it possible for PML to recognize and interact with other sumoylated proteins, including other sumoylated PML species (Song et al. 2004). PML has a stretch of amino acids which encode the nuclear localization signal (NLS). Here, the protein importin can bind to the NLS and this complex can further be transported from the cytoplasm into the nucleus through the nuclear pore complex (NPC) (Cokol et al. 2000; Lallemand-Breitenbach 2010). In this way, PML becomes actively imported into the nucleus.

1.3.1 PML nuclear bodies

In most cells, PML is mostly detected in the form of multiprotein complexes within the nucleus known as PML bodies (Bernardi & Pandolfi 2007; Ishov et al. 1999; Lallemand-Breitenbach 2010). These dynamic structures change their protein composition, morphology and location in a cell-cycle dependent manner. PML nuclear bodies (PML NBs) predominates in interphase cells. A normal cell typically contain 5 to 30 PML NB with a size of 0.2 to 1.0μm in diameter, dependent on cell type, cell-cycle phase and differentiation stage (Bernardi & Pandolfi 2007; Dellaire & Bazett-Jones 2004; Ishov et al. 1999). PML NBs are relatively immobile within the nucleus as a result of contact with chromatin (Eskiw et al. 2004), and their position are affected by chromatin modifications (Bernardi & Pandolfi 2007). In addition to PML, more than 100 other proteins have also been observed to co-localize with PML-NBs (Borden 2002; Chen et al. 2008). Examples of proteins that become recruited to PML bodies include the transcription regulator SP100 (Newhart et al. 2013), Fas death domain-associated protein (Daxx) which affect pro- and anti-apoptotic processes (Li et al. 2013) and SUMO (Bernardi & Pandolfi 2007). So far, PML is the only protein that is known to be required to form PML NBs. This is evident from analysis of *Pml*$^{-/-}$ cells, which fail to create PML NBs and leading to dispersed localization of other PML residence proteins (Ishov et al. 1999; Zhong et al. 2000a). The sumoylation-process have been proposed to be essential for PML to be able to form PML NBs (Shen et al. 2006; Zhong et al. 2000a). However, recent studies have shown that PML containing mutated

sumoylation sites are effective in forming PML bodies suggesting that sumoylation is not required (Cuchet et al. 2011; Lång et al. 2012).

1.3.2 PML and the cell cycle

During the cell cycle PML change morphology, biochemical composition and subcellular localization. This gives rise to different forms of PML bodies that varies in a cell cycle dependent manner (Figure 6). In interphase, PML proteins are in the form of PML NBs and are located inside the nucleus (Dellaire & Bazett-Jones 2004; Ishov et al. 1999). During S-phase, the number of PML NBs becomes about twice as many as in G_1 (Dellaire et al. 2006a). When a cell enters mitosis, PML start to aggregate into mitotic assemblies of PML proteins (MAPPs) and becomes de-sumoylated. Therefore, MAPPs do not associate with the same proteins as PML NBs and loose the interaction to chromatin and proteins such as SP100, Daxx and SUMO (Dellaire & Bazett-Jones 2004; Eskiw et al. 2004; Ishov et al. 1999). Palibrk et al. (2014) detected co-localization of MAPPs and early endosomes during mitosis. After mitosis, MAPPs remain in the cytoplasm, but complex with nucleoporins and transforms into cytoplasmic assemblies of PML and nucleoporins (CyPNs) in G_1 (Everett et al. 1999; Jul-Larsen et al. 2009). Nucleoporins (Nups) are components of the NPC, which functions as selective gates for transport of molecules in or out of the nucleus. PML complexes with several types of Nups, including Nup98 (Jul-Larsen et al. 2009). In this way, PML become recycled into the nucleus of the daughter cells and contributes to formation of new PML NBs.

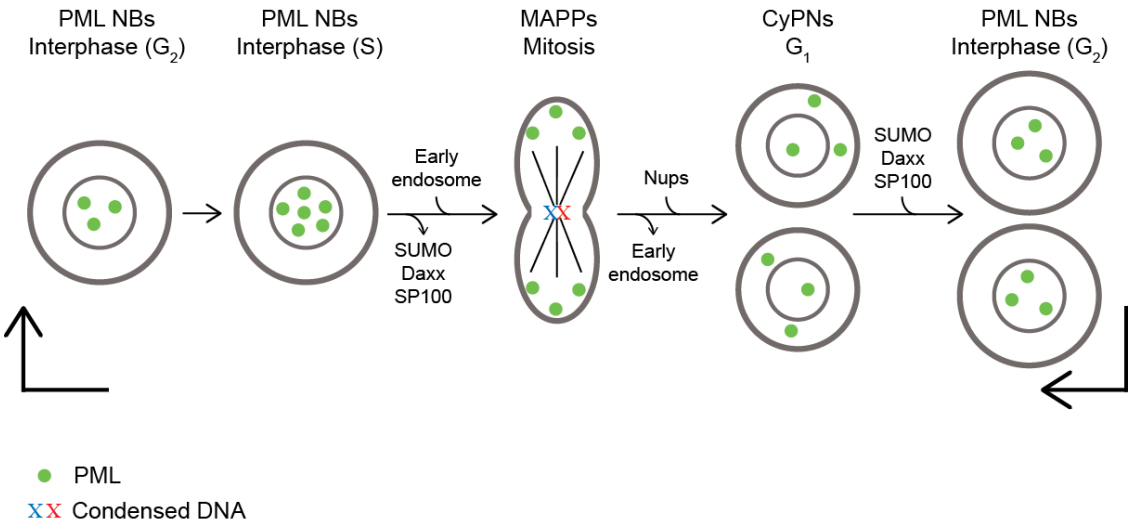

Figure 6. PML and the cell cycle. During cell cycle, PML changes location and association with different proteins and cell components. In interphase, PML is in the form of PML NBs in the nucleus and is associated with proteins such as SUMO, Daxx and SP100. The number of PML NBs increase during s-phase before entering mitosis. In mitosis, PML loose the interaction with SUMO, Daxx and SP100 at the same time as PML starts to aggregate into MAPPs. After mitosis, MAPPs remain in the cytoplasm, but complex with nucleoporins and transforms into CyPNs in G_1. Thereafter PML becomes recycled into the nucleus as PML NBs.

1.3.3 PML in development and differentiation

PML executes an important role in hematopoietic stem cell (HSC) maintenance by regulating asymmetric commitment of daughter cells after stem cell division (Ito et al. 2012). When present, PML regulates the signaling pathway that involves peroxisome proliferator-activated receptor δ-fatty-acid oxidation (PPARδ-FAO), which in turn leads to asymmetric HSC division. HSCs are located in the bone marrow and can differentiate into myeloid and lymphoid progenitors, which in turn will develop into B, T and NK-cells, or granulocytes, erythrocytes and platelets, respectively (Fuchs et al. 2004). There are several types of the nuclear receptors PPARs, where PPARδ has a role in transcriptional regulation of metabolic pathways, such as FAO (Braissant et al. 1996; Ito et al. 2012). Oxidation of fatty acids occurs in peroxisomes where the process shortens the fatty acid chain with two carbon atoms per cycle (Alberts et al. 2015). Ito et al. (2012) discovered that inhibition of FAO or deletion of *Pml* or *Ppard* would result in excessive symmetric HSC division and thus two differentiating daughter cells. It is not known if PML regulates asymmetric cell division in other cell types.

1.3.4 PML in mice

Although PML is essential in PML NBs, the protein is not fundamental for mice viability as *Pml*$^{-/-}$ mice are shown to be viable (Zhong et al. 2000a). *Pml*$^{-/-}$ mice are fertile, but often develop leukopenia as they have reduced levels of circulating granulocytes and myeloid cells (Wang, Z. G. et al. 1998). This in turn leads to increased susceptibility for infections and they may therefore have a reduced lifespan (Ing 1984; Lunardi et al. 2011; Wang, Z. G. et al. 1998).

PML appear to participate in apoptosis, as knockout mice do not perform programmed cell death at the same level as wildtype mice (Wang, Z.-G. et al. 1998; Zhong et al. 2000b). Caspases are proteases that perform a series of cleavage events that leads to targeted cell death (Alberts et al. 2015). *Pml*$^{-/-}$ mice do not react to caspase-dependent inducing signals such as Fas, tumor necrosis factor (TNF), ceramide, interferons and ionizing radiation (Wang, Z.-G. et al. 1998; Zhong et al. 2000b). Therefore, PML function as a pro-apoptotic factor and a tumor suppressor. This is supported by studies showing that knockout mice develop tumors after treatment with carcinogens at a higher frequency compared to wildtype controls (Wang, Z. G. et al. 1998).

During development of the mammalian brain, PML also contribute during neurogenesis and neuronal differentiation to make functional neurons (Ming & Song 2011; Regad et al. 2009).

As a consequence, loss of PML resulted in a smaller mouse brain and reduced size of the developing neocortex. A similar observation was made in mouse mammary glands, which undergo cellular growth, differentiation and cell death such as in periods related to pregnancy (Li et al. 2009). PML expression is shown to be regulated during these processes and affect progenitor cells that ultimately will contribute to the growth of mammary glands. Loss of PML resulted in aberrant differentiation of the mammary glands (Li et al. 2009). In addition, *Pml*$^{-/-}$ mice seem to have lower levels of anxiety-like behavior and developed abnormal memory and learning (Butler et al. 2013). These are some areas affected in *Pml*$^{-/-}$ mice, and highlights the fact that PML contributes in several biological processes and tissues.

1.3.5 Acute promyelocytic leukemia

The PML protein represents a target for treating acute promyelocytic leukemia (APL), a subtype of acute myelogenous leukemia (AML). APL constitutes about 10% of AML-cases in adults (Stone & Mayer 1990) and is caused by a reciprocal t(15;17) chromosome translocation between the gene encoding PML (chromosome 15) and that encoding the retinoic acid receptor α (RARA; chromosome 17). The t(15;17) translocation can be identified in more than 95% of APL patients and produces a fusion oncoprotein termed PML-RARA. The remaining APL cases contain translocation that involved the RARA gene fused to alternative genes, including promyelocytic-leukemia-zinc-finger (PLZF)-RARA, NuMA-RARA, nucleophosmin (NPM)-RARA and signal transducer and activator of transcription 5b (STAT5b)-RARA (Koken et al. 1997; Piazza et al. 2001; Puccetti & Ruthardt 2004). RARA contains a DNA binding site and functions as a transcription factor (Lång & Bøe 2011). The oncogenic fusion protein PML-RARA (Lanottei et al. 1990), however, acts as a transcription repressor upon binding to gene promoters. This inhibition is thought to hinder transcription of key genes that contributes to the differentiation of myeloid progenitors, thus inhibiting maturation of blood cells (Lång & Bøe 2011). The altered functions of PML and RARA generates severe bleeding tendency, accumulation of myeloid progenitors and cause APL (Jones & Saleem 1978).

Today, the effective therapeutic drugs arsenic trioxide (ATO) and all-*trans* retinoic acid (ATRA) are used to treat APL (Lång et al. 2012; Shen, Z.-X. et al. 1997). ATO interacts with the cysteine-rich motifs within the PML moiety of the PML/RARA oncoprotein, and causes sumoyation and ubiquitination (Zhang et al. 2010). This, in turn causes degradation of PML and PML/RARA by proteasome or autophagosome-dependent degradation pathways. This leads to elimination of the oncoprotein and subsequent differentiation of leukemic cells

followed by clinical remission (Lallemand-Breitenbach et al. 2008). Cells treated with low (< 0.5 μM) therapeutic relevant concentrations ATO generates more stable CyPNs after mitosis compared to CyPNs in untreated cells. In addition, the inhibition of PML and PML/RARA nuclear import causes an increase of cells containing CyPNs and a reduced number of PML NB after treatment with ATO (Lång et al. 2012). This contributes to how ATO promotes differentiation of APL cells (Lång et al. 2012).

ATRA interacts with the ligand binding site at the RARA moiety of the PML/RARA oncoprotein causing activation of the transcription machinery and therefore differentiation of blood cells (Lång & Bøe 2011; Nasr et al. 2008). ATRA combined with chemotherapy is found to be more effective than ATRA monotherapy (Chen et al. 1991; Lång & Bøe 2011). Moreover, synergistic treatment with both ATO and ATRA seems to treat APL even more effectively and with longer period for relapse free survival, especially for newly diagnosed APL cases (Estey et al. 2006; Shen et al. 2004). This might be explained that both ATO and ATRA cause degradation of the oncogenic protein and that they act on each of the two moieties of PML/RARA (Lång & Bøe 2011). The mechanisms behind the successful clinical treatment of APL are of interest as this knowledge might be transferred to other variants of cancers. Therefore, further research on APL, ATO, ATRA and its associated proteins, drugs and mechanisms is vital.

1.4 Goals of this study

PML is a tumor suppressor protein involved in several cellular functions including apoptosis, senescence, differentiation, genome maintenance and virus defense (Bernardi & Pandolfi 2007; Grignani et al. 1993; Salomoni et al. 2008; Wang, Z. G. et al. 1998). PML is associated with APL as more than 95% of the cases are caused by the t(15;17) translocation between PML and RARA. However, APL can be effectively treated with the therapeutic drugs ATO and ATRA that in turn will degrade the oncoprotein (Lång et al. 2012; Shen, Z.-X. et al. 1997). The protein forms PML bodies, which are located inside the interphase nucleus. More than 100 proteins are found to co-localize with PML bodies, including Daxx, SUMO and SP100 (Borden 2002; Chen et al. 2008). During the cell cycle PML change morphology, subcellular localization and protein composition (Dellaire & Bazett-Jones 2004; Everett et al. 1999; Ishov et al. 1999). During mitosis, PML is in the form of MAPPs, while PML co-localizes with nucleoporins and

generates CyPNs after mitosis before PML NBs are re-generated in the nucleus (Everett et al. 1999; Jul-Larsen et al. 2009).

PML bodies are inherited by the daughter cells after mitosis. Thus, PML bodies have large potential of becoming asymmetrically distributed during mitosis. Asymmetric PML body partitioning may contribute to differentiation. A recent, unpublished study (Lång et al. Unpublished 2016) have shown that PML bodies become asymmetrically distributed in human keratinocytes in culture. In this thesis, we wanted to investigate if the mitotic and early G_1 distribution of PML bodies in mouse epidermis and cultured mouse keratinocytes and fibroblasts was asymmetric. Mouse embryonic tissue was chosen for these studies as PML is highly expressed in the basal cells and as the mouse is frequently used as an experimental model organism.

The PML bodies were seen to become distributed to both daughter cells in all analyzed samples in mice epidermis and in cultured MEKs and MEFs. This symmetric segregation differs from complete asymmetric segregation that occurs in human keratinocytes (Lång et al. Unpublished 2016) and suggests that different mechanisms are utilized for the distribution of PML bodies in mice and humans. The role of PML bodies in mouse epidermis during embryonic development was further analyzed by measuring the angle of the cell division in $Pml^{+/+}$ and $Pml^{-/-}$ epidermis. The PML depleted mice tends to have a more random orientation of the cell division compared to PML wildtype, and that could indicate that PML may therefore contribute in the development of epidermis. PML was also found to aggregate in mitotic MEKs, and the number of PML bodies became fewer as PML became stabilized as CyPNs after treatment with ATO in MEFs and HDFs.

The experimental approach was as follows:

1. Surgically isolate pups, process by paraffin embedding
2. Section paraffin embedded mice embryos at embryonic stages E15.5 and E17.5 ($Pml^{+/+}$ and $Pml^{-/-}$)
3. Perform immunohistochemistry (IHC) with desired antibodies and visualize samples by confocal microscopy
4. Isolate mouse epidermal keratinocytes ($Pml^{+/+}$ and $Pml^{-/-}$) from one-day old mice skin
5. Cultivate keratinocytes ($Pml^{+/+}$ and $Pml^{-/-}$) and fibroblasts ($Pml^{+/+}$) of mouse origin

6. Cultivate and treat mouse epidermal fibroblasts ($Pml^{+/+}$) and human dermal fibroblasts ($Pml^{+/+}$) with ATO
7. Perform immunofluorescence (IF) on cultivated cells with desired antibodies before visualization by confocal microscopy
8. Identify pairs of newly divided daughter cells, determine the ration of asymmetric PML body distribution

2 Materials

2.1 Animal strains and cell lines

Animal strains and cell lines	**Supplier**
Human dermal fibroblasts (HDF) (C-013-5C)	Gibco
Mouse epidermal fibroblasts (MEF)	Isolated by Rajikala Suganthan (MIK, OUS)
Mouse epidermal keratinocytes (MEK)	Isolated by Ingrid Olstad and Anna Połeć
Pml$^{-/-}$ mice (129/Sv-PML^{tm1Ppp})	Crossbreeding between 129 PML KO against C57BL/6N for at least 8 generations (Wang, Z. G. et al. 1998)
Pml$^{+/+}$ mice (C57BL/6N)	Provided by Magnar Bjørås (OUS)

2.2 Chemicals

Chemicals	**Supplier**
Arsenic trioxide (ATO) As_2O_3 (202673)	Sigma Aldrich
4',6-diamidino-2-phenylindole (DAPI) $C_{16}H_{15}N_5 \cdot 2HCl$ (D3571)	ThermoFisher Scientific
Dimethyl sulfoxide (DMSO) C_2H_6OS ≥99.9% (D8418)	Sigma Aldrich
Ethanol 100%, C_2H_5OH (absolute alcohol prima)	Kemetyl Norge AS
Ethanol 75%, C_2H_5OH (600642)	Antibac AS
Ethanol 96%, C_2H_5OH (rectified alcohol)	Kemetyl Norge AS
Formalin 10% (CHE/BAF-0010-25A)	Chemi-Teknik AS
Glycerol ≥99% $C_3H_8O_3$ (G-5516)	Sigma Aldrich
HEPES 1M $C_8H_{18}N_2O_4S$ pH7.0	Microbiological department OUS
Hydrogen chloride 37%, HCl (20252.290)	VWR
Immersol (518 F)	Carl Zeiss Jena GmbH
Nail polish	Hennes & Mauritz
Neo-Clear® Xylene substitute (1.09843.5000)	Merch Millipore

Paraformaldehyde 98% (PFA) $HO(CH_2O)nH$ (15,812-7)	Sigma Aldrich
Penicillin/Streptomycin 10000U/ml (Pen/Strep) (DE17-602E)	LONZA
Sodium chloride ≥98%, NaCl (3014)	Sigma Aldrich
Trisodium-citrate dihydrate, $C_6H_5Na_3O_7.2H_2O$ (71404)	Sigma Aldrich
Triton X-100 (T8787)	Sigma Aldrich
Trypan Blue Stain 0.4% (T10282)	Life technologies
Tween20 pH=6 (P9416)	Sigma Aldrich
Vectashield antifade mounting medium with DAPI (H-1200)	Vector laboratories

2.3 Media supplements

Media supplements	**Supplier**
10x Phosphate buffered saline (PBS)	Microbiology department OUS
Bovine serum albumin (BSA) 30% in DPBS (A9576)	Sigma Aldrich
CnT-Prime (CnT-PR)	CELLnT
Collagen I, bovine protein 5ml/mg (A10644-01)	Gibco
Collagen IV, human placenta (C7521)	Sigma Aldrich
Defined trypsin inhibitor (R-007-100)	Gibco
DispaseII (D4693)	Sigma Aldrich
Dulbecco's Modified Eagle Medium (DMEM) (high glucose 4500 mg/L (1x) (31053-044)	Gibco
Dulbecco's PBS (DPBS) (1x) (14190-136)	Gibco
Epidermal growth factor (EGF) >97% (236-EG)	R & D systems
Fetal bovine serum (FBS) non-USA origin (F7524)	Sigma Aldrich
Fetal bovine serum (FBS), certified, US origin (160000)	Thermo Fisher
Fibronectin bovine protein (33010-018)	Gibco
Goat serum (GS) (G9023)	Sigma Aldrich
HDF EpiLife medium (MEP1500CA)	Gibco
Heparin sodium salt from porcine intestinal mucosa (H3149-25KU)	Sigma Aldrich
Hydrocortisone $C_{21}H_{30}O_5$ (H0888)	Sigma Aldrich
L-glutamine (GlutaMAX) (100x) (35050-087)	Gibco

Non-Essential Amino Acids Solution (MEM) (100x) (11140035)	Gibco
Soybean trypsin inhibitor (M191-1G)	VWR
Trypsin-EDTA solution (1x) (R-001-100)	Gibco
Trypsin-EDTA solution (T4049)	Sigma Aldrich

2.4 Media

Mouse keratinocytes growth medium:

CnT-Prime containing the following supplement:

1:100 Pen/Strep

Mouse fibroblasts growth medium:

DMEM containing the following supplements:

10% (v/v) FBS heat inactivated for 30 min at 56ºC

2mM L-glutamine (GlutaMAX)

1:100 MEM

1:100 Pen/Strep

Human dermal fibroblasts growth medium:

HDF EpiLife medium containing the following supplements:

2% fetal bovine serum (chelex-treated FBS)

1µg/ml hydrocortisone

10mg/ml epidermal growth factor (EGF) >97%

3ng/ml heparin

1:100 Pen/Strep

2.5 Stock solutions

HCl 1M:

8.3ml 37% HCl

91.7ml MQ

Mixed to a 100ml stock

NaOH 1M:

4.0g NaOH

100ml MQ

Antigen retrieval buffer:

2.49g trisodium-citrate dihydrat

1000ml MQ

500µl Tween20

Mixed to a 1000ml stock and adjusted to pH6 with 1M HCl before addition of Tween20

Washing buffer:

900ml MQ

100ml 10xPBS

500µl Tween20

Mixed to a 1000ml stock

Blocking buffer:

15.6ml 1xPBS

1ml GS

3.4ml 30% BSA

Mixed to a 20ml stock and aliquoted into 1.5ml Eppendorf tubes, stored in -20ºC

Staining buffer:

1.5ml blocking buffer

13.5ml 1xPBS

Mixed to a 15ml stock.

Collagen coating for MEK:

Collagen IV

CnT medium

20mg/ml of Collagen IV in CnT medium

DispaseII (5U/ml):

1ml Hepes

19ml MQ sterilized through 0.2µm filter

0.175g NaCl

0.2g DispaseII

Adjusted pH with NaOH until pH=7.5. Diluted 1:1 with CnT medium with 2 x Pen/Strep to a final concentration of 2.5U/ml

Cryopreservation media for MEKs:

2.4ml DMSO

9.6ml CnT medium

Mixed to a 12ml stock, stored in 4ºC

Soybean trypsin inhibitor:

2mg Soybean trypsin inhibitor

1ml DPBS

2:1 dilution of soybean trypsin inhibitor and DPBS. Filtered through 0.2µm pores before usage

Cryopreservation media for MEFs and HDFs:

6ml DMEM or HDF growth medium

2ml DMSO

2ml FBS

Medium and DMSO was mixed inn before addition of FBS for a 10ml solution

Collagen coating for MEFs and HDFs:

1ml of 1mg/ml fibronectin

1ml of 3mg/ml collagen I

0.5ml 2% BSA in 1xPBS

2ml 1M HEPES

For 100ml of medium. Filtered through 0.2µm pores before usage

4% PFA in PBS:

160ml 1xPBS

8g PFA

1M NaOH

1xPBS was preheated up to ~80ºC before PFA was added. Raised the pH slowly by addition of 1M NaOH until the solution cleared. Adjusted the volume to 200ml by adding 1xPBS and adjusted pH to 6.9

0.25% TritonX-100 in 1xPBS:

25µl TritonX-100

9,975ml 1xPBS

Mixed for a 10ml stock

2.6 Antibodies

Primary antibodies	**Supplier**
Anti-AuroraB rabbit polyclonal antibody (AuroraB (rabbit)) (ab2254)	Abcam®
Anti-cytokeratin 5 mouse monoclonal (K5 (mouse)) (ab190083)	Abcam®
Anti-cytokeratin 5, rabbit polyclonal (K5 (rabbit)) (ab24647)	Abcam®
Anti-Nup98 antibody rat monoclonal [2H10] (Nup98 (rat)) (ab50610)	Abcam®
Anti-PML (PG-M3) mouse monoclonal antibody (PML (PG-M3)) (sc-966)	Santa Cruz Biotechnology
Anti-PML mouse monoclonal antibody (PML (mouse)) (05-718)	Merch Millipore

Secondary antibodies	**Supplier**
Alexa Fluor ® 488 (A488) goat anti-mouse (A-11029)	ThermoFisher Scientific
Alexa Fluor ® 555 (A555) goat anti-rat (A-21434)	ThermoFisher Scientific
Alexa Fluor ® 594 (A594) goat anti-rabbit (A-11072)	ThermoFisher Scientific

2.7 Laboratory equipment

Laboratory equipment	**Supplier**
24 well plate Nunclon™ Delta Surface	Thermo Scientific
60mm cell culture dish Nunclon™ Delta Surface	Thermo Scientific
Cell culture flasks with vented cap, Nunc™ EasYFlask™ with Nuncleon™ Delta Surface, 25cm^2 (T25), 75cm^2 (T75), 175cm^2 (T175)	Thermo Scientific
Cell strainer 40µm nylon, 70µm nylon	FALCON
Countess™ cell counting chamber slide	Invitrogen™
Cover slip 18x18mm	VWR
22x22mm	MARIENFELD SUPERIOR
Cryo freezing container, NALGENE® Mr. Frosty™	Thermo Scientific
CryoTube™ Vials 1.8ml	ThermoFisher Scientific
Daco pen, PAP hydrophobic barrier pen	Abcam®
Eppendorf tubes 1.5ml	Eppendorf
Falcon 50ml with flat base, 15ml and 50ml with round base	SARSDEDT
Glass bottom microwell dishes, 3mm petri dish and 14mm microwell	MatTec corporation
Glass coverslips 12mm	VWR
Immunoslide staining tray	Pyramid Innovation
Microscope slides SuperFrost®Plus	VWR
Parafilm	Bemis®
Pipette tips of various size	SARSTEDT
Serological pipettes 2ml, 5ml, 10ml, 25ml	SARSTEDT
Staining tray	Pyramid Innovation
Sterile filters 0.20µm pore size	SARSTEDT
Syringe 10ml, 50ml	BD Plastipak™
Thermanox ® Plastic Coverslips, cell cultured on one side	Nalge Nunc international
Various pipettes	ThermoFisher Scientific

2.8 Instruments

Instruments	Supplier
-80ºC freezer	Thermo Scientific
Centrifuge Megafuge 1.0	Heraeus
Countess™ automated cell counter	Incitrogen™
Flow hood: Holten LaminAir Model 1.2	Thermo Scientific
Hot plate	BEHA HEDO
Ice flaker machine Metos	Brema Ice Makers
Incubators: BINDER	BINDER
FORMA STERI-CYCLE CO_2	Thermo Scientific
Hybridization oven	Amersham Pharmacia Biotech
Microscopes: confocal TCS SP8 with 40x oil immersion lens	Leica
Primovert light microscope	Zeiss
Microtome	Thermo Scientific
Microwave oven	KENWOOD
MilliQ PLUS	Merch Millipore
pH-meter MR3000	Heidolph
Pressure cooker 6L	Function
VORTEX-GENIE 2	Scientific Industries
Water bath OLS 200	GRANT
Weight	METTLER TOLEDO

2.9 Software

Software	Supplier
Adobe Illustrator CC (version 2015)	Adobe
Adobe Photoshop CE 7.0 (version 6.2)	Adobe
GraphPad InStat3 (version 3.1)	GraphPad
GraphPad Prism (version 7)	GraphPad
ImageJ (version 1.5)	National Institutes of Health
R (version 3.2.3)	The R Project

3 Methods

3.1 *In vivo* model

Research on mice have given valuable information that is transferrable to humans and can contribute to develop diagnostic methods and treatments of human diseases. The mouse is ideal as a model as the genome is comparable to humans, they are easy to breed and have a short generation time (Frick et al. 2013).

3.1.1 Isolation of the material

We used mouse as an *in vivo* model to investigate PML in mitotic cells in basal layer of epidermis. All experiments were performed according to ethical regulations by Mattilsynet and all requirements were fulfilled. Application for animal experiments were submitted and approved in Forsøksdyrforvaltningens tilsyns- og søknadssystem (FOTS) with the project number 6390. Person responsible for performing animal experiments was Anna Połeć. For *in vivo* experiments, mice embryos were obtained at the developmental stages E15.5 and E17.5 based on protocol from Lichti et al. (2008). After isolation, whole embryos were washed with 75% ethanol followed by DBPS and set into 4% PFA before 10% formalin. Thereafter the embryos were subjected for fixation in order to perform dehydration and paraffin embedding for sectioning (Abcam 2013/2014; Thavarajah et al. 2012).

3.1.2 Immunohistochemistry (IHC)

IHC is a method for visualization of components (e.g. proteins) in cells within a tissue section by use of specific antibodies binding to antigens in biological tissues. For indirect immunofluorescence (IF), the secondary antibody is usually linked to a fluorochrome that causes the antigens in the tissue to emit light at a specific wavelength in a fluorescence microscope. Indirect IF was performed by using a protocol from Abcam® (Abcam 2013/2014). Briefly, tissues were cut in thin sections and mounted to microscope slides. The antigen retrieval process removes paraffin and gradually hydrates the tissue. Thereafter immunohistochemical staining was performed by first blocking of all epitopes to prevent unspecific binding of secondary antibodies and therefore reduce background noise. Primary antibodies are designed to bind desired epitopes in tissues while secondary antibodies bind primary antibodies. A fluorochrome is conjugated to the secondary antibody and after excitation by a laser, emitted light can be detected in a confocal microscope.

Performance

1. Microscope slides were put in a metal rack and placed into an incubator for 10 min at 57-58ºC.
2. Thereafter the following samples were subjected to rehydration as follows:
    a. Neo-Clear 2 x 5 min
    b. Ethanol 100% 2 x 3 min
    c. Ethanol 96% 1 min
    d. Ethanol 75% 1 min
    e. Kept slides in MQ until antigen retrieval was performed and made sure the tissues did not dry
3. Antigen retrieval was performed in a pressure cooker for 2.5 min in the presence of approximately 2L of antigen retrieval buffer. The pressure cooker was opened and slowly filled with cold tap water for 10 min to cool down the tissues.
4. Thereafter the slides were put in washing buffer for 5 min.
5. Carefully wiped around the tissues to remove as much liquid as possible and used a Daco hydrophobisity pen to draw a circle around the tissue.
6. Blocking and staining with primary and secondary antibodies were conducted in a lightproof staining tray. The environment was kept humid by distributing a small amount of MQ in the tray. 80µl of blocking buffer was applied to each tissue sample and incubated for 30 min at room temperature (RT).
7. The tissues were then washed with washing buffer 3 x 5 min.
8. Primary antibodies were added to staining buffer before 80µl was applied to each tissue sample and incubated overnight at 4ºC.
9. Next day, the tissues were washed with washing buffer 3 x 5 min.
10. Secondary antibodies were diluted in staining buffer before 80µl of the dilution was applied to each tissue sample. Thereafter, the samples were incubated for 2h at 37ºC.
11. After the incubation with primary and secondary antibodies, the tissues were washed with washing buffer 3 x 5 min at RT.
12. DAPI was diluted in staining buffer (1:1000) and 80µl was then applied to each tissue before a 5 min incubation at RT.
13. The tissue samples were briefly washed with washing buffer before 12µl of Vectashield mounting medium was applied. Cover slips were placed on top of the samples and nail

polish was used to secure the corners of the cover slips. The samples were analyzed by confocal microscopy (section 3.3).

Primary and secondary antibodies used in IHC

The primary and secondary antibodies that were used for staining embryonic tissues are listed below. The used antibodies and their concentrations are listed (Table 1).

Table 1. Primary and secondary antibodies used in IHC. Overview of primary and secondary antibodies with their respective dilution ratios.

Primary antibodies:	**Secondary antibodies:**
Anti-PML (mouse) 1:400	A488 (goat anti-mouse) 1:500
Anti-K5 (rabbit) 1:500	A594 (goat anti-rabbit) 1:500

3.2 *In vitro* cell culture model

Cell lines can be obtained from commercial manufactures or they can be isolated from living tissue samples. Cells in culture can be propagated to large numbers, and they can be stimulated by different factors, chemicals or drugs before evaluating the effect in cell cultures. Cell cultures can behave differently compared to cells in tissue due to differences in physiological conditions. Still, cell culture experiments gives valuable information, are easy to manipulate and have high reproducibility. Different types of cells and different cell lines have various culture conditions, they can be cryopreserved for long-term storage and thawed to re-seed cells into culture. When cells reach confluence of ~70-90%, they must be subjected to passaging to retain viability and phenotype. However, prolonged passaging can result in senescence, a cell state where the cultured cells stop growing. In this thesis, MEKs and MEFs were used for experiments between passage 1 and 3 while HDFs was used between passages 4 to 9.

Before working with live cells, equipment was sterilized by treatment with soap and 75% ethanol or microwaving for 2-3 min to hinder infections. Solutions for MEKs had to become pre-warmed to room temperature before working with the cells.

3.2.1 Isolation of primary cells from tissue

MEKs

One-day old mice pups were handled according to regulations previously described in section 3.1.1. Keratinocytes were isolated from the skin of one-day old pups according to protocol from CellnTec (CellnTec).

1. Skin was obtained from one-day old pups. The fat layer and muscle residues were removed and the skin was cut in approximately 0.5cm x 1cm pieces.
2. About 5 pieces of 0.5cm x 1cm skin were transferred to a 15ml tube containing 5ml of 1 x dispase II with antibiotics. Made sure all pieces were submerged in the solution and stored overnight (~15h) at 4ºC.
3. Next morning, the pieces of skin were placed in a petri dish with CnT medium, epidermal side up. The epidermal layer was peeled off from the dermis by using forceps and all pieces were collected in one 15ml tube with DPBS.
4. The pieces of epidermis were centrifuged at 180 x *g* for 5 min at RT.
5. Thereafter, the pieces were transferred to a new 15ml tube with ~1ml trypsin-EDTA solution and incubated for ~4 min in water bath at 37ºC.
6. To release the cells from epidermis, the solution was pipetted ~20 times before filtration through a 70µm cell strainer into a 50ml falcon tube. Equal volume of soybean trypsin inhibitor to the volume of trypsin used, was quickly added to neutralize the trypsin.
7. The solution was again centrifuged at 180 x *g* for 5 min at RT.
8. The supernatant was carefully removed and the cell pellet was resuspended in 1ml CnT medium.
9. The number of cells was counted in a Countess™ automated cell counter by mixing 15µl of cells in 1ml medium and 15µl of Trypan Blue Stain. 10µl of the solution was then placed on each side of the Countess™ cell counting chamber slide before viability and number of cells were estimated.
10. Cells were seeded on collagen IV treated T-tanks and 60mm cell culture dishes with surface treated plastic cover slips. The collagen IV treatment lasted for 30 min before culture vessels and culture dishes became briefly washed with DPBS and stored in CnT medium until seeding of the cells.
11. Cells were then incubated for three days at 37ºC with 5% CO_2.
12. After that, the media was changed every two or three days by letting ~1ml of old media remain in the culture vessel and by adding fresh media relative to the culture vessels

size and 60mm cell culture dish. It may take 7-10 days before the cells start to proliferate at a higher rate.

3.2.2 Preservation of cell lines

The procedures of splitting, cryopreservation and thawing MEKs followed the protocol from CellnTec (CellnTec), while procedures for MEFs and HDFs were based on ThermoFisher (2009). CnT medium was used for MEKs while DMEM was applied for MEFs and EpiLife-medium was used for HDFs. When cells reached a confluence of 70-90%, they were splitted to a new passage or cryopreserved. Cells were seeded in new culture flasks, 24-well plates and/or 60mm culture dishes with coverslips, glass coverslips for MEFs and HDFs while MEKs were seeded on surface treated plastic coverslips. When the 60mm culture dishes reached confluence of 70-90%, IF was performed as described in section 3.2.4.

Passaging of cells

1. Confluent cells were washed twice with DPBS before trypsin-EDTA solution (from Gibco and Sigma) was added to the culture vessel. After brief washing, 1-3ml of trypsin-EDTA solution was immediately removed before the culture vessel with the remaining trypsin was incubated for 4 min at 37ºC with 5% CO_2.
2. After the incubation period, cells were checked for detachment in a light microscope. The culture vessel was tapped strongly to release the remaining cells.
3. The cells were quickly transferred to a 50ml falcon tube with equal volume of trypsin inhibitor. The culture vessel were rinsed with media to collect all cells.
4. The solution was centrifuged at 180 x *g* for 5 min at RT before the supernatant was decanted and the cell pellet resuspended in 1ml medium according to cell type. The number of cells were counted in a Countess^{TM} automated cell counter as described in section 3.2.1 and seeded on collagen treated (collagen IV for MEKs, collagen I/fibronectin for MEFs and HDFs) culture vessels and/or 60mm cell culture dishes with coverslips. Cells were incubated at 37ºC with 5% CO_2.
5. The following day, cells were washed twice with DPBS before addition of fresh medium. Thereafter the medium was changed every two to three days until confluence of 70-90% was achieved.

Cryopreservation of cells

1. First, the desired amount of cryo-vials were labeled and placed in a cryo freezing container (Mr. Frosty^{TM}) at -18ºC.
2. Confluent cells were detached from their culture vessels as described in the protocol for passaging of cells (section 3.2.2).
3. After centrifugation at 180 x *g* for 5 min at RT, the pellet was resuspended in 1ml medium, put on ice and performed a cell count as described in section 3.2.1.
4. For MEKs, the desired final concentration of cells was 1 x 10^6 cells/ml, therefore the concentration of the MEKs was adjusted to 2 x 10^6 cells/ml with CnT medium. Thereafter, same amount of cold (4ºC) freezing medium was slowly added dropwise while mixing to make a 1:1 ratio between MEKs in CnT medium and freezing medium. For MEFs and HDFs, freezing medium was slowly added drop by drop in a 1:10 ratio of cells to freezing medium.
5. The cells stood for 5 min on ice before 1ml of the solution became transferred to the pre-cooled cryo-vials in the freezing container. The cells were stored overnight up to one week in -80ºC and then transferred into liquid nitrogen for long-term storage.

Thawing of cells

1. Prepared collagen or collagen/fibronectin coated culture vessels and/or 60mm culture dishes with coverslips according to cell type for 30 min. Thereafter the culture vessels were washed twice with DPBS and stored in medium.
2. Vials containing cells were collected from the nitrogen tank and transported on dry ice. Thereafter the vials were rapidly thawed in a 37ºC water bath and made sure that the temperature of the cells did not rise above 4ºC and that some ice crystals were left.
3. For MEKs, cells were resuspended by using a 1ml pipette and counted as previously described. Thereafter, the cells were directly transferred to the culture vessels containing CnT medium. Unlike, MEFs and HDFs were transferred to a 50ml falcon tube before dropwise addition of ~9ml of medium according to cell type. MEFs and HDFs were centrifuged at 180 x *g* for 5 min at RT. Thereafter the supernatant was decanted, the cells resuspended in 10ml DPBS and set for centrifugation. After the supernatant was removed, cells were resuspended in 1ml medium. Cells were counted as previously described and seeded in culture vessels with appropriate media before incubation at 37ºC with 5% CO_2.

4. The medium for MEKs was changed after 12-24h while the incubation of MEFs and HDFs were not disturbed for the first 72h. Subsequently, the medium was changed every two to three days until confluence of 70-90% was achieved.

3.2.3 Cell treatment

ATO

1. Confluent MEFs and HDFs cultured on glass coverslips in 24-well plates were washed twice with 0.5ml DPBS.
2. ATO was added to DMEM and HDF medium to a final concentration of 0.25µM. Wells with MEFs and HDFs were added normal medium for the untreated control and medium with 0.25µM ATO for the ATO-treated samples. One of the 24-well plates was set up for 4h incubation while the other 24-well plate was incubated for 24h at 37ºC with 5% CO_2.
3. After the incubation period, cells were fixated and immunofluorescence (IF) was performed as described in section 3.2.4.

3.2.4 Immunofluorescence (IF)

IF was performed on cells cultured in 60mm culture dishes and in 24-well plates when confluence was reached. The cells were fixated and permeabilized before immunostaining was performed with primary- and conjugated secondary antibodies to detect desired antigens. The IF procedure was based on Jul-Larsen et al. (2004) with some modifications.

Protocol

1. Confluent cells cultured on coverslips were washed twice with DPBS before fixation with 4% PFA for 10 min.
2. Thereafter, cells were permeabilized for 4 min with 0.25% Triton X-100 in 1xPBS and then washed twice with 1xPBS. Cells can be stored in 1xPBS in 4ºC for later use or proceeded directly to the blocking step.
3. The following blocking and staining with primary and secondary antibodies were conducted in a lightproof staining tray. The environment was kept humid with tissue paper soaked in MQ. 60µl of blocking buffer was pipetted dropwise on parafilm before the coverslips were placed onto the blocking buffer, cells facing down, for 15 min at RT.

4. Blocking buffer was diluted in 1xPBS to make a staining buffer before primary antibodies were added. Each sample was placed onto 60µl of staining buffer and incubated overnight at 4ºC.
5. The next morning, samples were washed twice with 1xPBS for 4 min before 60µl of staining buffer with secondary antibodies were added and incubated for 2h at 37ºC.
6. Thereafter, cells were washed three times with 1xPBS for 4 min before DAPI diluted in staining buffer (1:1000) was added to the samples and incubated for 5 min at RT.
7. Cells were then briefly washed with 1xPBS, mounted with 12µl Vectashield mounting medium to object glasses, cells facing down, and secured the corners with nail polish. Then samples were analyzed by confocal microscopy (section 3.3).

Primary and secondary antibodies used in IF

The primary and secondary antibodies that were used for staining cultured cells are listed below. The used antibodies and their concentrations are listed with specification for the cell lines (Table 2).

Table 2 Primary and secondary antibodies used in IF. Overview of primary and secondary antibodies with their respective dilution ratios.

Primary antibodies	Secondary antibodies
MEK	
Anti-AuroraB (rabbit) 1:200	A594 (goat anti-rabbit) 1:500
Anti-PML (mouse) 1:400	A488 (goat anti-mouse) 1:500
MEF	
Anti-AuroraB (rabbit) 1:200	A594 (goat anti-rabbit) 1:500
Anti-Nup98 (rat) 1:100	A555 (goat anti-rat) 1:500
Anti-PML (mouse) 1:400	A488 (goat anti-mouse) 1:500
HDF	
Anti-AuroraB (rabbit) 1:200	A594 (goat anti-rabbit) 1:500
Anti-Nup98 (rat) 1:100	A555 (goat anti-rat) 1:500
Anti-PML PG-M3 (mouse) 1:200	A488 (goat anti-mouse) 1:500

3.3 Confocal microscopy

Visualization of cells were carried out using a Leica TCS SP8 confocal microscope with a 40x oil immersion lens. About 15 to 25 z-sections that covered the entire cell were generated to complete an image. In the *in vivo* experiment, late mitotic and early G_1 cells were analyzed in three to four embryos of the same age. The cells were analyzed for presence of PML bodies in the cells. The DAPI staining was used for detecting the chromatin during mitosis. For the *in vitro* experiments, Anti-AuroraB was used as a marker for cells in cytokinesis or early G_1 phase of the cell cycle. Non mitotic cells were left out from the analysis. Random cells were scanned for immunofluorescently labeled cells with Anti-Nup98.

3.4 Data analysis

3.4.1 Image analysis

Images from the confocal microscope of mitotic cells for the *in vivo* and *in vitro* experiments were analyzed in ImageJ. For quantification of PML bodies, a line was drawn between the two daughter nuclei before the number of PML bodies in the cytoplasm was manually counted in each daughter cell. In sections of mice embryos, the angle of the cell division was measured by drawing a line parallel to the basement membrane in epidermis and another line through the center of the daughter cells nuclei. Thereafter an angle measure tool in ImageJ was used. Angles $\leq 30^{o}$ were defined as horizontal cell divisions, angles between 30^{o} and 60^{o} as oblique cell divisions and angles $\geq 60^{o}$ as vertical cell divisions. Data was plotted into Inc. (2016) to make rose diagrams. The area of PML bodies in the cytoplasm of mitotic MEKs and in the nucleus of interphase MEKs was measured. This was performed by using an area-measure tool in ImageJ, which was drawn close around the PML bodies. In MEFs and HDFs, the number of PML was counted and CyPNs were scored when PML accumulated to nucleoporins in control and ATO-treated cells.

3.4.2 Statistical analyses

Dr. Alexander Rowe performed the simulation of the distribution of PML bodies in daughter cells in R. The data was grouped to visualize the distribution of the PML bodies in each group. Thereafter, the ratio of PML bodies in daughter cells was determined by dividing the PML rich cell by the PML poor cell. Then, the definition of symmetric and asymmetric distribution was determined by simulating 2000 bimodal distributions. The simulations were then plotted onto the raw data to detect the most appropriate level of asymmetry. Chi-squared tests of

independence were used for comparing the angles of cell divisions in tissues. The data was grouped into three different sets of angles (((≤30º, >30º<60º, ≥60º) and quantified the amount of angles in each group. Thereafter the tests were performed with two degrees of freedom in GraphPad InStat. The tests were then repeated in R with guidance from Dr. Xianwen Chen, giving the same results as in GraphPad InStat. Unpaired student t-tests were performed using Microsoft Excel for the analysis of aggregation of PML bodies in mitotic and interphase MEKs, in addition to the comparison of control and ATO-treated cells in MEFs and HDFs. A p-value <0.05 was considered statistically significant.

4 Results

4.1 PML in mice epidermis

Mice embryos were sectioned at the embryonic stages E15.5 and E17.5 before IHC was performed and visualized by confocal microscopy. Figure 7 displays representative images for PML wildtype stages E15.5 and E17.5. Staining with K5 is detected in the basal layer, which cells are dominant in epidermis at E15.5. In addition, a high amount of PML is expressed in the basal cells compared to the upper K5 negative layer. The periderm, which protects the epidermis is also found to react with the K5 antibody. At E17.5, epidermis is almost fully developed and PML expression is elevated in the basal cells. At that stage, the periderm has started to disappear, as it will be replaced with layers of stratified cells from the stratum corneum.

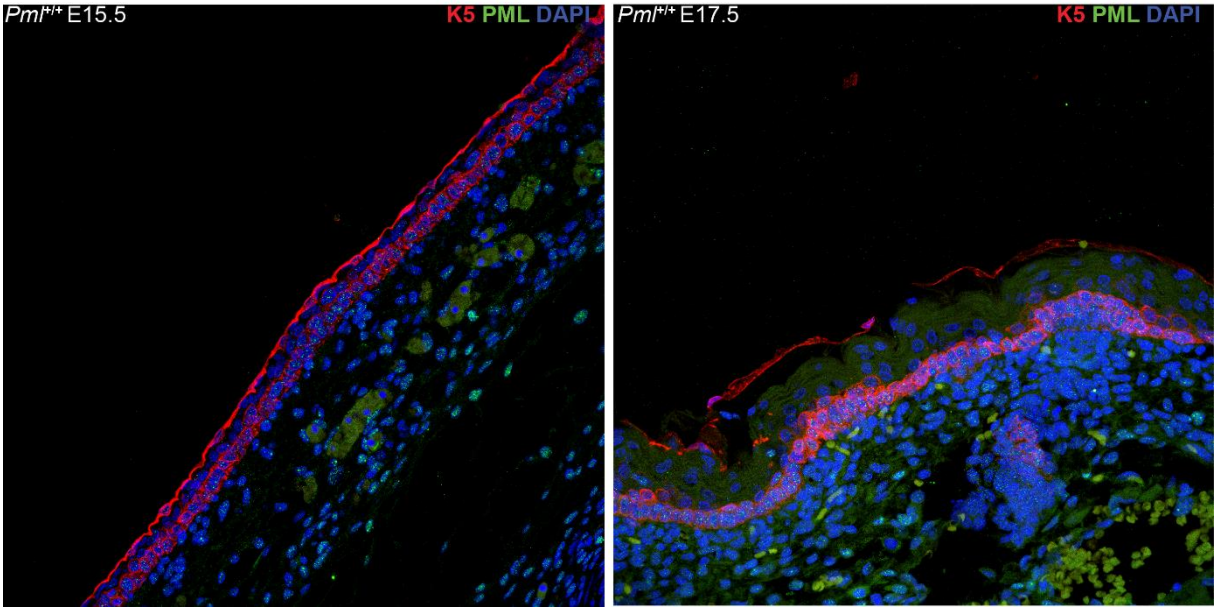

Figure 7. Expression of PML in mice epidermis at the embryonic stages E15.5 and E17.5. Mice embryos were paraffin embedded, cut and mounted to microscope slides before IHC was performed and visualizaed by confocal microscopy. Sections were stained with antibodies against K5 as basal keratinocyte marker (red) and PML (green), while DAPI (blue) was used for detection of chromatin. PML is highly expressed in the basal cells of epidermis at both embryonic stages. Images represent projections of multiple z-sections.

4.1.1 Symmetric distribution of PML NBs in mitotic basal cells in mice epidermis

An essential part of the data analysis in this thesis was to identify cells in late mitosis and cytokinesis, both *in vivo* and *in vitro*, and quantify the inherited PML NBs in each daughter cell. To achieve this we first drew a line in the middle of the two daughter cells before PML NBs present in the cytoplasm were manually counted (Figure 8). The cell with the most PML NBs was designated as PML rich and the daughter cell with the least amount of PML NBs as PML poor (Figure 8 and Figure 9).

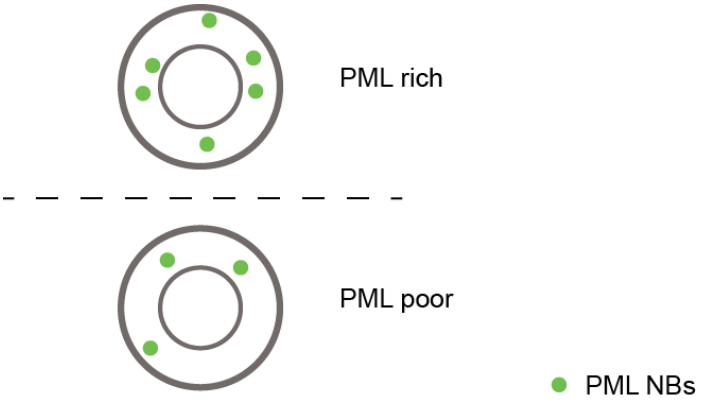

Figure 8. How PML NBs were counted in mitotic and cytokinetic cells. Late mitotic cells (anaphase/telophase) and cells in cytokinesis were identified in basal cells in mice epidermis at the embryonic stages E15.5 and E17.5. A line was drawn between the two daughter cells with the same distance to the nucleus. The daughter cell with most PML NBs was identified as PML rich and the daughter cell with least PML NBs as PML poor. The inner grey circle represents the nuclear membrane while the outer circle defines the cell membrane.

PML NBs were manually counted in mitotic basal cells in PML wildtype epidermis at E15.5 and E17.5 (Figure 9A). PML depleted mice were used as a control. Figure 9B visualizes the counted PML NBs in each daughter cell pair in PML wildtype basal cells. For those cell pairs inspected, every daughter cell inherited PML NBs revealing a symmetric distribution of PML bodies in mice.

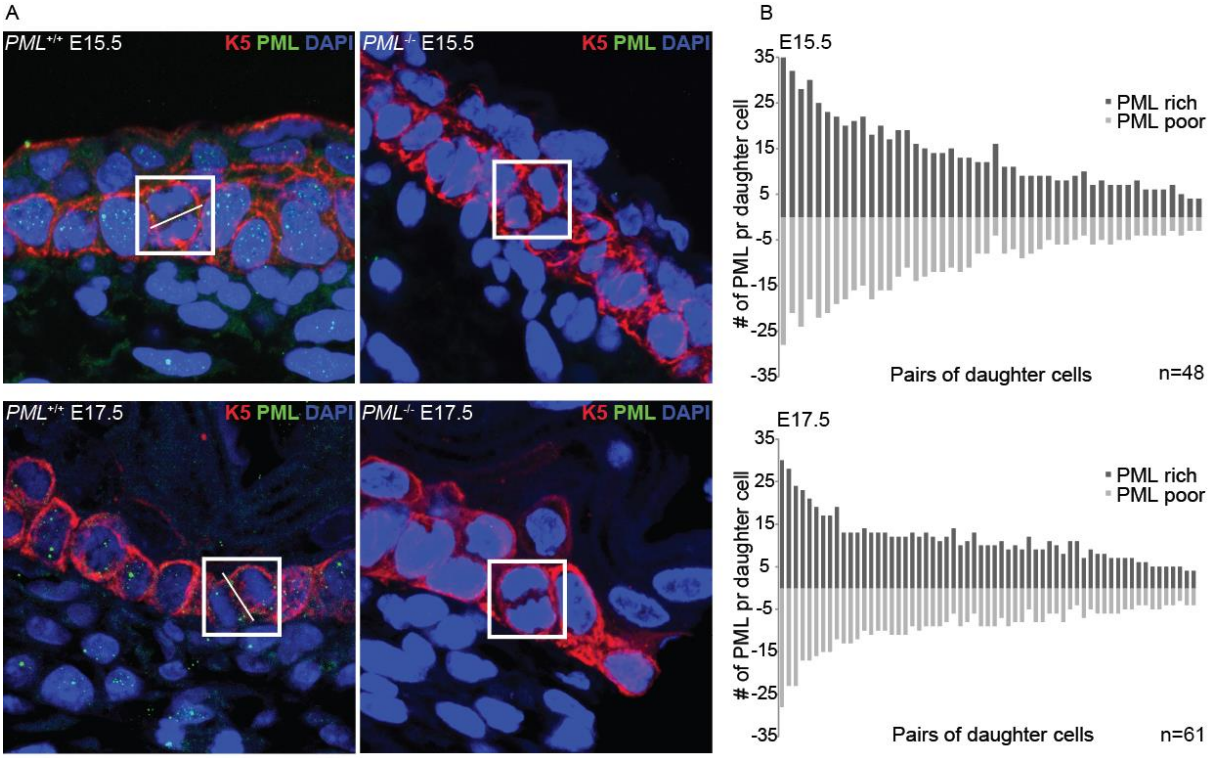

Figure 9. Mitotic cells in the basal layer of mice epidermis. Mice at embryonic stages E15.5 and E17.5 were paraffin embedded, cut and mounted to microscope slides. IHC staining was performed and samples were visualized by confocal microscopy. Both $Pml^{+/+}$ and $Pml^{-/-}$ sections were stained with antibodies against K5 (red) and PML (green), while DAPI (blue) was used for detection of chromatin. (A) Mitotic cells in the basal layer are highlighted with a white square and a line is drawn in the middle of the nuclei to define the cytoplasmic area to each daughter cell. Images represent projections of multiple z-sections. (B) Mitotic distribution of PML NBs. The daughter cell with most PML NBs is referred to as PML rich while the other daughter cell with the least inherited PML NBs as PML poor. PML bodies were manually counted in late mitotic cells (anaphase/telophase) and cells in cytokinesis.

Statistical simulations were performed to analyze the distribution of PML bodies in tissue. The ratio of PML bodies in daughter cells was determined by dividing the largest PML body count by the smallest PML body count in the daughters. Then, the definition of symmetric and asymmetric distribution was determined by simulating 2000 bimodal distributions (Figure 10) before the simulated values were plotted over the curves for both E15.5 and E17.5 (Figure 11). The distribution of PML bodies in both E15.5 and in E17.5 was most similar to the yellow line, which indicates complete symmetric distribution of PML bodies in daughter cells in mice epidermis.

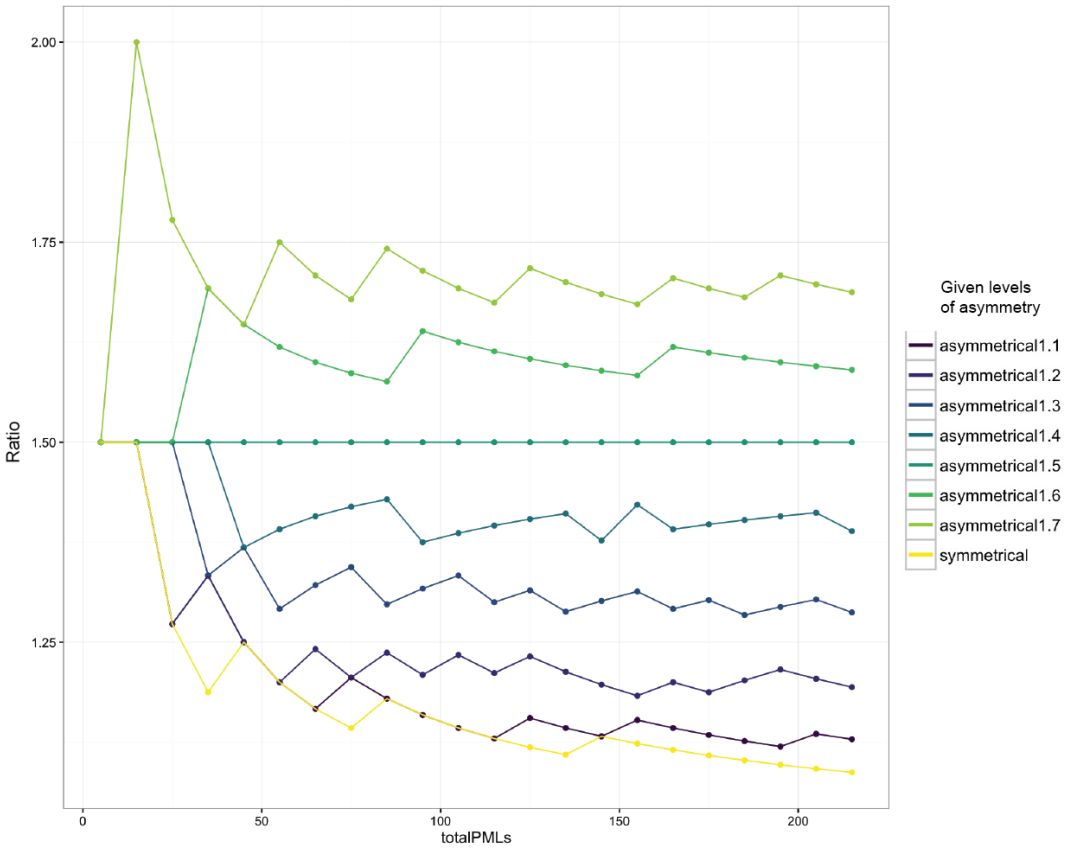

Figure 10. Simulated ratios of PML bodies between daughter cells depending upon a given level of asymmetry. Each point was calculated from 2000 repeat of random samples of the asymmetric distribution model, including sorting into high and low values as in the real experiments. The ratio was determined by dividing the largest PML body count by the smallest PML body count. The different levels of asymmetry was characterized as asymmetrical 1.1 through 1.7 in addition to the complete symmetrical line (yellow). The asymmetries are as follows with the average low percentage listed before the average high percentage: 1.1 (0.50, 0.50), 1.1 (0.48, 0.52), 1.2 (0.45, 0.54), 1.3 (0.43, 0.57), 1.4 (0.42, 0.58), 1.5 (0.40, 0.60), 1.6 (0.38, 0.62) and 1.7 (0.38, 0.62).

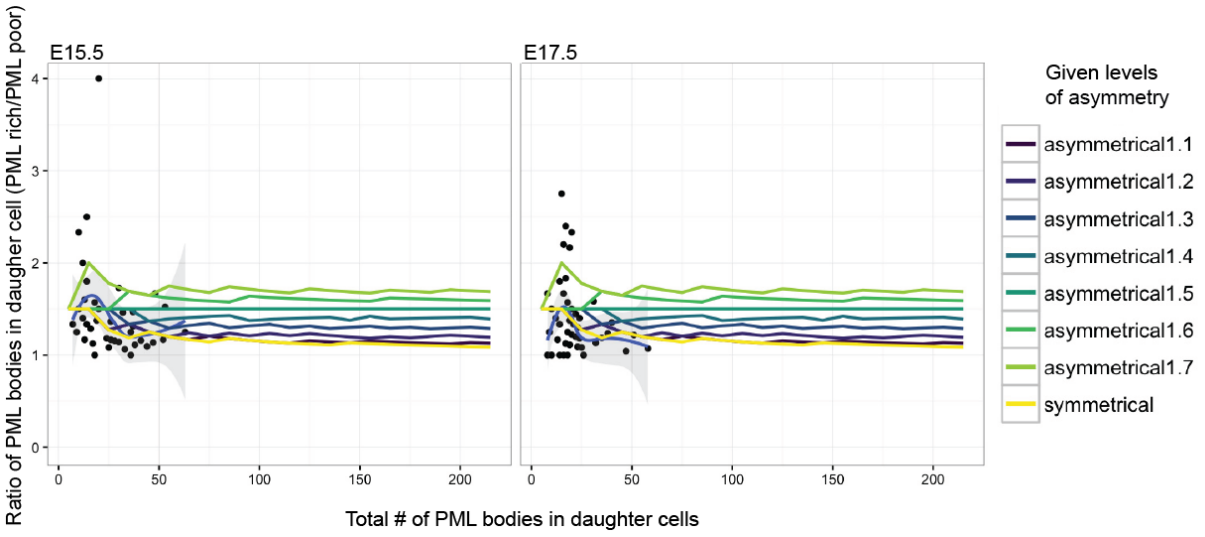

Figure 11. Simulations of asymmetry plotted over the results for the distribution of PML bodies between daughter cells in mice epidermis. The short blue line represents the real data, while the grey ribbon is the 95% confidence interval. The data from E15.5 (n=48) and E17.5 (n=61) are almost identical to the yellow line, which indicates total symmetry. The values of the given asymmetries are as follows with the average low percentage listed before the average high percentage: 1.1 (0.50, 0.50), 1.1 (0.48, 0.52), 1.2 (0.45, 0.54), 1.3 (0.43, 0.57), 1.4 (0.42, 0.58), 1.5 (0.40, 0.60), 1.6 (0.38, 0.62) and 1.7 (0.38, 0.62).

4.1.2 Orientation of the cell division in mitotic basal cells in mice epidermis

In the following experiments, the angle of the cell divisions was measured in mitotic basal cells in mice epidermis. Both PML wildtype and PML depleted cells were investigated in order to determine if PML depletion affects cell division orientation (Figure 12). PML depleted cells seemed to have a more randomized mitosis angle distribution compared to the wildtype cells. However, no statistical differences were found (Table 3; chi-squared test of independence with two degrees of freedom) based on the data. Statistically significant differences between PML wildtype and PML depleted cells may have been obtained if sample number had been larger.

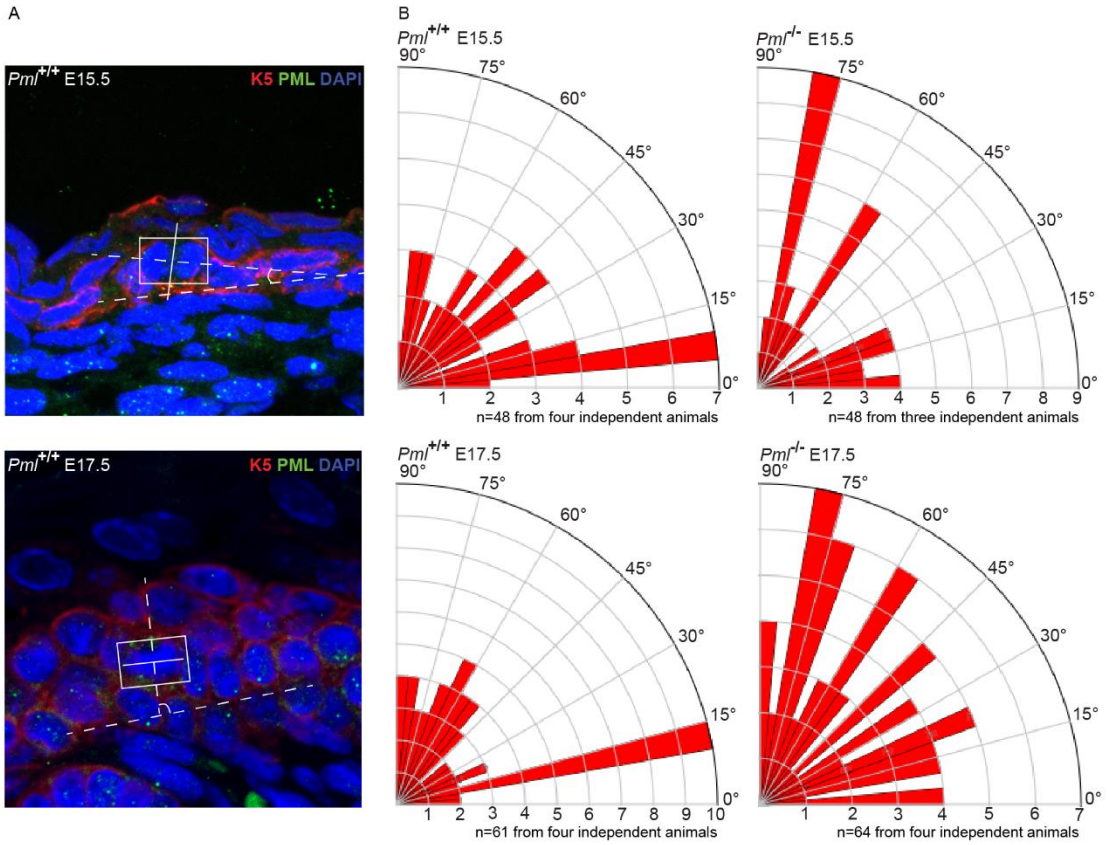

Figure 12. The angle of mitotic cell division in relation to the basement membrane of mice epidermis. *Pml*$^{+/+}$ and *Pml*$^{-/-}$ mice at embryonic stages E15.5 and E17.5 were paraffin embedded, cut and mounted to microscope slides before IHC was performed and samples were visualized by confocal microscopy. Sections were stained with antibodies against K5 (red) and PML (green), while DAPI (blue) was used for detection of chromatin. (A) First, a line (solid) was drawn in the middle of the two daughter nuclei at late mitosis (E15.5) or lengthwise through a metaphase cell (E17.5). Next, the angle was determined by drawing a line (dashed) parallel to the basement membrane and another line (dashed) through the mitotic daughter nuclei at 90º of the first solid line. Thereafter, an angle measure tool in ImageJ was used. A cell division angle of 0º indicated complete horizontal orientation of the cell division relative to the basement membrane. Images represent projections of multiple z-sections. (B) Rose diagrams depicting the orientation of cell division. The number of segments indicates the number of mitotic cell divisions at each measured angle (≤30º=horizontal cell division, >30º-<60º=oblique cell division, ≥60º=vertical cell division). P values were identified by Chi-square test of independence (Table 3), no significant results were found.

Table 3. P-values from chi-square test of independence when comparing the angle of cell division in mice epidermis. P-values are listed from comparing PML wildtype and PML depleted cells at E15.5 and E17.5, in order to determine if there is a difference between the two embryonic stages or if PML depletion affects cell division orientation. No significant results were found.

Condition 1	Condition 2	Chi-square p-value	Significance
E15.5 *Pml*$^{+/+}$	E17.5 *Pml*$^{+/+}$	0.2419	n.s.
E15.5 *Pml*$^{+/+}$	E15.5 *Pml*$^{-/-}$	0.1427	n.s.
E17.5 *Pml*$^{+/+}$	E17.5 *Pml*$^{-/-}$	0.8199	n.s.
E15.5 *Pml*$^{-/-}$	E17.5 *Pml*$^{-/-}$	0.4297	n.s.

4.2 PML in cultured MEKs and MEFs

4.2.1 Symmetric distribution of PML in mitotic MEKs and MEFs

The distribution of PML NBs was further investigated *in vitro* in cultured MEKs and MEFs. AuroraB was used as a marker for late mitosis and newly divided cells before a line was drawn in the middle of the two daughter nuclei and PML NBs present in the cytoplasm were manually counted in each daughter cell. PML depleted cells were used as control. Figure 13 represents the different cell cycle stages that were used to quantify the PML NBs.

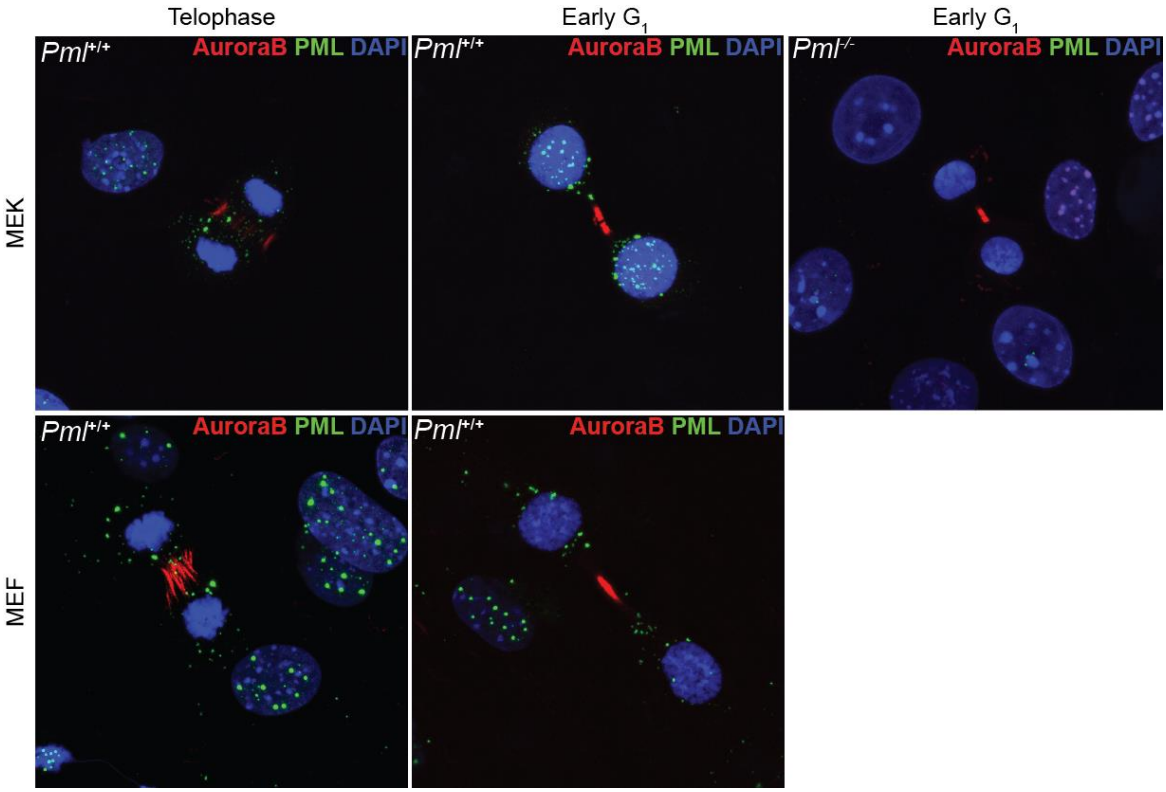

Figure 13. PML in telophase and early G$_1$. MEKs and MEFs were cultured on coverslips until ~70% confluence, then fixated and permeabilized. IF was performed and samples were visualized by confocal microscopy. *Pml*$^{+/+}$ and *Pml*$^{-/-}$ cells were visualized at different stages of the cell cycle, telophase and early G$_1$, respectively. Cells were stained with AuroraB (red) to identify pairs of newly divided daughter cells, PML (green) and chromatin with DAPI (blue). Images represent projections of multiple z-sections.

All daughter cell pair investigated in MEK and MEF cell cultures inherited PML NBs. The distribution of these structures in each cell pair is depicted in Graph 1. The same simulation of symmetry vs. asymmetry was performed on the cultured cells (Figure 14) with the identical levels of asymmetry as shown in Figure 10. The distributions of PML bodies in MEKs and MEFs resembled level 1.3 the most of the given levels of asymmetry, meaning an approximate 40-60% segregation of the bodies. This level is quite close to complete symmetric distribution of PML bodies and the distribution was therefore determined as symmetric in MEKs and MEFs.

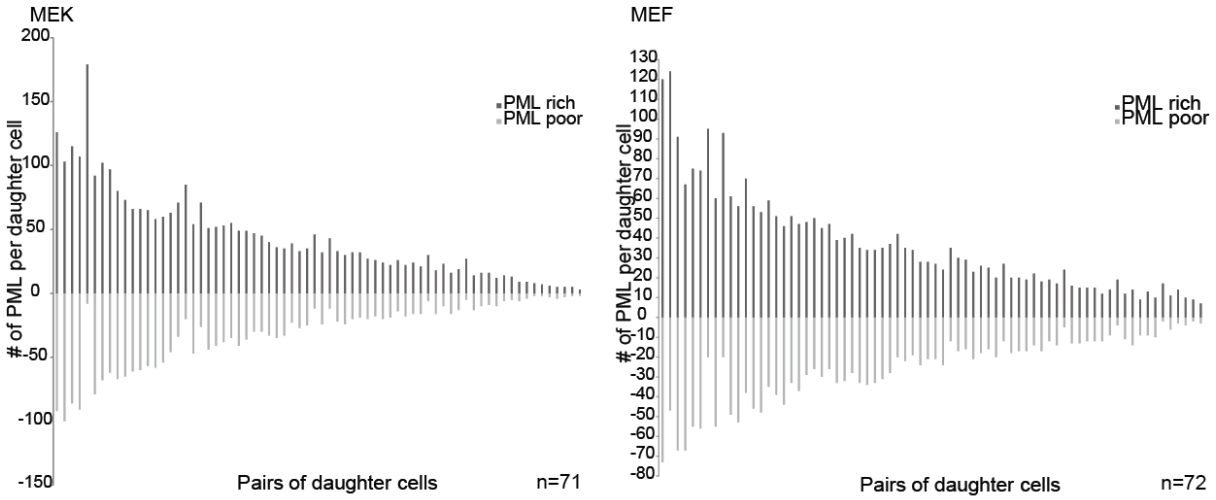

Graph 1. Symmetric distribution of PML bodies in mitotic MEKs and MEFs. MEKs and MEFs were cultured on coverslips until ~70% confluence, then fixated and permeabilized. IF was performed and samples were visualized by confocal microscopy. Cells were stained with AuroraB (red) to detect pairs of daughter cells, PML (green) and chromatin with DAPI (blue). PML was manually counted in each daughter cell.

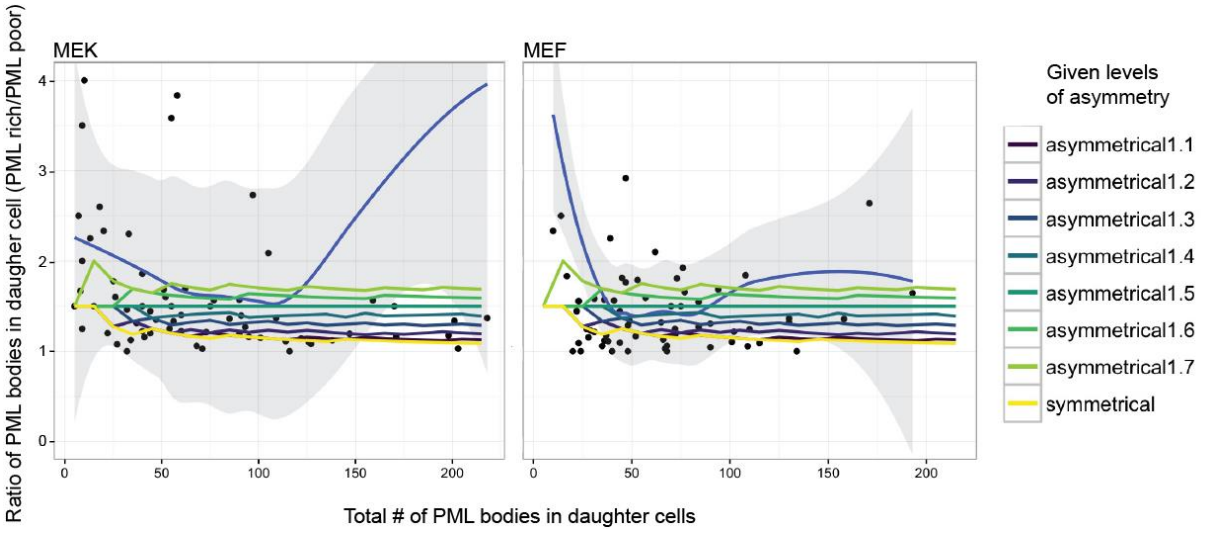

Figure 14. Simulations of asymmetry plotted over the results for the distribution of PML bodies between daughter cells in cultured cells. The blue line represents the real data, while the grey ribbon is the 95% confidence interval. The data for MEK (n=71) and MEF (n=72) resembles level 1.3 the most. The values of the given asymmetries are as follows with the average low percentage listed before the average high percentage: 1.1 (0.50, 0.50), 1.1 (0.48, 0.52), 1.2 (0.45, 0.54), 1.3 (0.43, 0.57), 1.4 (0.42, 0.58), 1.5 (0.40, 0.60), 1.6 (0.38, 0.62) and 1.7 (0.38, 0.62).

4.2.2 Aggregation of PML in mitotic MEKs

In human cells, the PML bodies have been shown to aggregate into larger structures following entry into mitosis. To investigate if aggregation also occurs in mouse cells, the area of PML bodies was measured in the interphase nucleus and in the cytoplasm of mitotic MEKs (Figure 15). This was done by measuring the area of the four largest PML bodies in six mitotic and ten interphase cells. An unpaired t-test showed that PML bodies in interphase nucleus are significantly smaller than PML bodies detected in mitotic cells (Figure 15; p=0.0005). This result shows that PML bodies in MEKs is subjected to aggregation upon entry into mitosis.

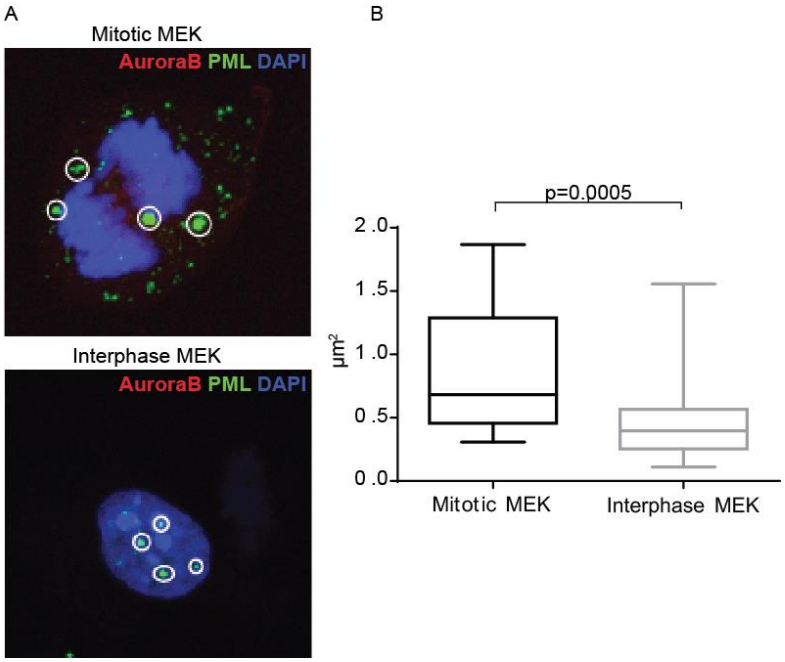

Figure 15. PML aggregates in mitotic MEKs. MEKs were cultured on coverslips until ~70% confluence, then fixated and permeabilized before IF was performed with antibodies against AuroraB and PML. DAPI was used to visualize the nuclei. (A) The area of the four largest (represented by white circles) PML was measured in six mitotic and ten interphase MEKs. Images represent projections of multiple z-sections. (B) Box-plots depicting the values of the measured area in mitotic and interphase MEKs. An unpaired t-test shows that PML bodies in interphase nucleus are significantly smaller than PML bodies detected in mitotic cells.

4.3 PML and Nup98 co-localizes within CyPNs after treatment with ATO

Earlier studies have detected co-localization of PML and nucleoporins in the cytoplasm after treatment with ATO (Lång et al. 2012). To investigate if PML and nucleoporins respond to ATO in a similar way also in mouse cells, we performed IF on MEFs and HDFs using antibodies against PML and the nucleoporin Nup98. Figure 16 represents images of cultured MEFs and HDFs cells grown in normal medium as a control and in medium containing 0.25µM ATO for 4 and 24h.

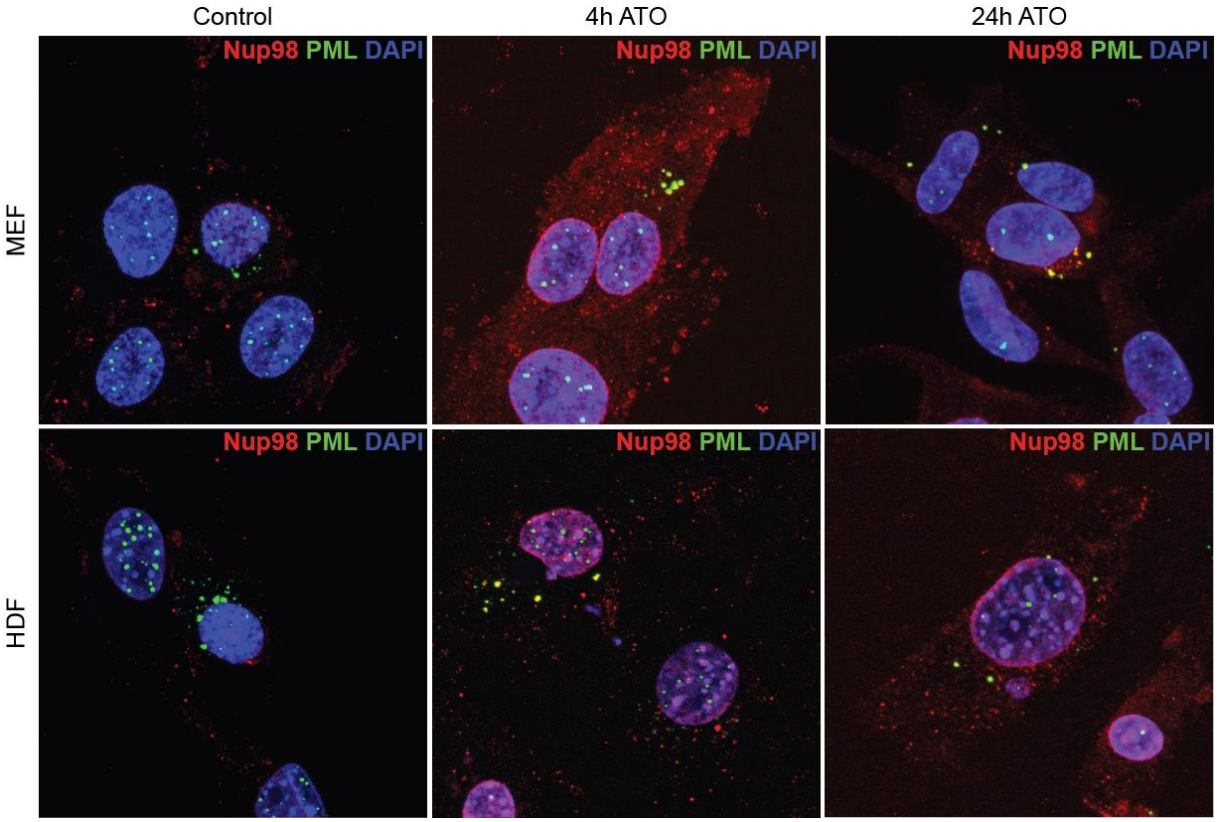

Figure 16. Co-localization of PML and Nup98 in CyPNs after treatment with ATO. MEFs and HDFs were cultured in medium with or without 0.25µM ATO for 4 and 24h. After fixation and permeabilization, IF was performed with antibodies against Nup98 (red) and PML (green). DAPI is shown in blue to visualize the nuclei. Cells were thereafter imaged by confocal microscopy. Images represent projections of multiple z-sections.

The number of cytplasmic PML NBs and CyPNs where PML NBs co-localized with Nup98 were manually counted in each randomly selected cell (Graph 2). The number of PML NBs becomes reduced according to the length of ATO-treatment in both cell types concomitant with the stabilization of CyPNs by ATO. Further, the number of CyPNs per cell was highest after 4h treatment. An unpaired t-test was performed between the control and treated cells. Significant and non-significant results are depicted in Graph 2.

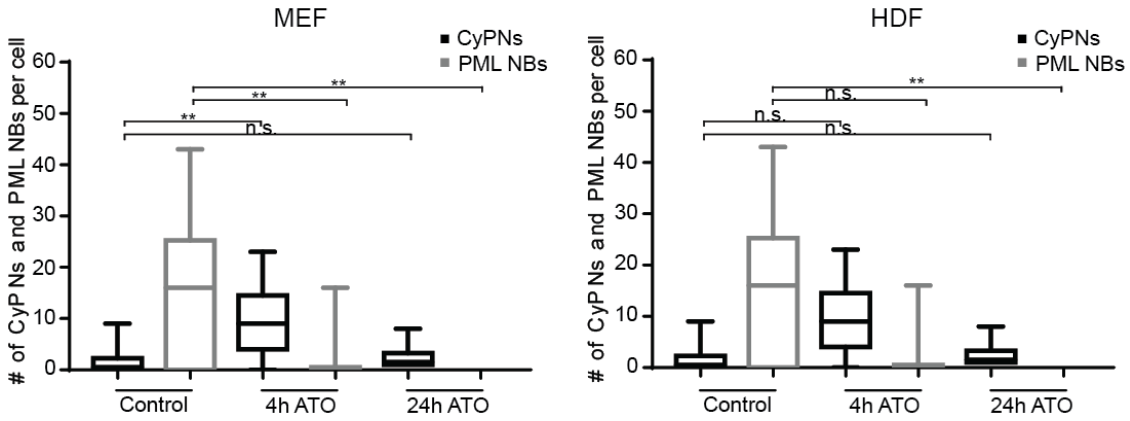

Graph 2. ATO treatment induce CyPN-formation in MEFs and HDFs. MEFs and HDFs were cultured in medium with or without 0.25μM ATO for 4 and 24h. After fixation and permeabilization, IF was performed with antibodies against Nup98 (red) and PML (green), while DAPI (blue) was used for detection of chromatin Cells were thereafter imaged by confocal microscopy. The number of CyPNs and PML were manually counted in each cell. Number of cells analyzed was between 10 and 13 for each group. An unpaired t-test was performed between the control cells and treated cells for 4 and 24h (n.s. = $p>0.05$, ** = $p\leq0.01$).

5 Discussion

The skin covers the surface of the body and protects against unwanted influences from the environment, and against dehydration and pathogenic bacteria (Forni et al. 2012; Hsu et al. 2014; Koster & Roop 2007). The epidermis comprises the outermost layers of the skin with proliferating basal and differentiating suprabasal cells. APL is caused by the t(15;17) translocation between the gene encoding PML and RARA. This translocation hinders transcription of genes related to the maturation of myeloid progenitors and therefore inhibits the maturation of blood cells (Lanottei et al. 1990; Lång & Bøe 2011). In healthy cells, PML can function as a tumor suppressor and participate in several cellular processes including apoptosis, senescence, differentiation, genome maintenance and virus defense (Bernardi & Pandolfi 2007; Grignani et al. 1993; Salomoni et al. 2008; Wang, Z. G. et al. 1998).

The data presented in this thesis emphasizes the role of PML NBs in cell divisions in mice epidermis. In the late 1980s, ATRA was for the first time given to APL-patients and resulted in the discovery of differentiation of leukemic promyelocytes in patients with better long-term prospectives compared to chemotherapy treatment (Wang & Chen 2008). This discovery was an inspiration to explore the mechanisms behind APL. ATO and ATRA were later found to participate in degradation of the PML-RARA oncoprotein leading to clinical remission. Still, the mechanisms behind these clinical treatments have not been completely elucidated. For example, the role of PML NBs partitioning during mitosis for APL therapy is incompletely understood. Epidermis consists of a basal layer and suprabasal layers including spinous layer, granular layer and the uppermost stratum corneum. The cell turnover is relatively high in the skin, and stem cells in the basal layer divides and can differentiate as they migrate towards the suprabasal layers (Blanpain & Fuchs 2009; Candi et al. 2005; Forni et al. 2012; Koster & Roop 2007). In the present thesis we find that basal cells in mice epidermis have a high expression of PML and contain a relatively high number of PML NBs. This result is in agreement with unpublished results by Emma Lång, who observed high expression of PML in basal layers of human epidermis (Lång et al. Unpublished 2016). However, the number and fluorescence intensity of PML bodies does not persist within differentiated cells present in the suprabasal layers. Therefore, it is important to understand the mechanisms that regulates the expression of PML bodies in the skin.

5.1 Symmetric distribution of PML NBs in mice epidermis and in cultured MEKs and MEFs

Mice epidermis was chosen as an *in vivo* model to study distribution of PML in mitotic cells. Several aspects make the epidermis a suitable model. First, during mice embryonic development, PML bodies becomes highly expressed in epidermal basal cells, especially at E15.5. Second, there are well established methods for visualization of different stages in skin development during embryonic development in sectioned tissue. These methods are cheap and give reproducible results. In addition, mice have been widely used as an experimental model for tissue development and a lot of information about skin structure, function and development is available in the literature.

Cell division is important for the development and maintenance of the epidermis. Symmetric cell divisions generate two daughter cells with the same fate, while asymmetric cell divisions generate cells with different fates, such as one self-renewing basal cell and one differentiating cell (Blanpain & Fuchs 2009; Doe 1996; Horvitz & Herskowitz 1992). The mechanisms controlling the switch between symmetric and asymmetric cell division is incompletely understood and needs to be further investigated.

The PML bodies were seen to become distributed to both daughter cells in all analyzed samples in mice epidermis and in cultured MEKs and MEFs (Figure 9 and Graph 1). Different given levels of asymmetry was defined and plotted over the data from epidermis and MEKs and MEFs. The distribution of PML bodies in epidermis followed a complete symmetric segregation, while MEKs and MEFs were classified for asymmetrical level 1.3 (Figure 11 and Figure 14). This level resembles a ratio of 40-60% distribution between the daughter cells and as this level is so close to 50-50%, the distribution of PML bodies were classified as symmetric in MEKs and MEFs. This result is in contrast to unpublished results by Lång et al. (Unpublished 2016) showing that PML bodies in human keratinocytes are distributed completely asymmetric among daughter cells in more than 25% of the cell divisions.

MEKs are the same cell type as those analyzed in sectioned samples of epidermis, and were therefore expected to give similar results. However, MEKs were analyzed at a later stage in development as they were isolated from one-day old pups compared to the epidermis that was analyzed from embryos. In addition, we were able to analyze a larger number of cell divisions

in cultured MEKs compared to epidermal cells in tissue. *In vivo* and *in vitro* experiments can have altered results when compared, such as MEKs had no space limitation that constrains cell division and may therefore develop slightly different compared to cells in tissue. Based on these studies, we concluded that PML bodies predominantly becomes symmetrically distributed in MEKs and MEFs.

This differs from what was recently observed in cultured human keratinocytes where more than 25% of the of the mitotic cells displayed complete asymmetric distribution of PML bodies (Lång et al. Unpublished 2016). When asymmetric segregation occur in human cultured keratinocytes, the PML bodies had a tendency of accumulating to one side of the nucleus in prophase (Lång et al. Unpublished 2016). Therefore, PML might be actively recruited to this side of the cell before segregation into one of the daughters. How PML bodies become asymmetrically segregated in human keratinocytes and how this affects cell fates of the daughters are interesting questions. The Par-complex in *Drosophila* neuroblasts segregates apically during asymmetric cell division (Betschinger & Knoblich 2004; Dewey et al. 2015; Goldstein & Macara 2007; Knoblich 2008). This complex generates cell polarity that induces cell fate determinants, such as Numb, to segregate basally. Numb inhibits Notch signaling and therefore hinder the newly divided basal cell to self-renew, but differentiate into a GMC-cell that will ultimately divide into two neurons (Doe 1992; Knoblich 2008; Wang et al. 2006). This asymmetric accumulation of Numb affects the fates of both daughter cells. Possibly, a similar mechanism might apply for PML bodies in human cultured keratinocytes as the PML bodies are asymmetrically distributed between daughters and are highly expressed in the basal cells in epidermis. Absence of PML bodies in the other daughter cell might therefore contribute to the differentiation into a spinous cell. In this way, asymmetric segregation of PML bodies could participate in development and maintenance of epidermis.

As PML bodies constantly were observed to become inherited by both daughter cells in mice epidermis, there needs to exist a mechanism to distribute the PML bodies to both daughters in a symmetrical fashion. Devenport et al. (2011) discovered that components contributing to cell polarity in mouse epidermis were selectively internalized into endosomes during mitosis. They proposed that the interaction with endosomes during cell division facilitated equal inheritance of planar cell polarity (PCP) proteins by daughter cells. This could also be a possible mechanism for symmetric distribution of PML bodies in basal cells in mice. In agreement with this, Palibrk

et al. (2014) discovered that PML bodies forms stable interactions with early endosomes during mitosis.

Despite the lack of asymmetric PML body inheritance during division of basal keratinocytes in mice, the daughter cells that develops into suprabasal cells seems to have down regulated PML expression. One possible mechanism that can inhibit translation or induce degradation of messenger RNA (mRNA), is the non-coding microRNAs (miRNA) (Selbach et al. 2008). Distinct miRNAs are already known to have a role in self-renewal, proliferation and differentiation of mouse epidermis (Shenoy & Blelloch 2014). The result of PML expression in mice epidermis might be equal as in human skin, although the pathway during mitosis may differ. Still, mechanisms generating symmetric segregation of PML bodies in mice and how this affects cell fates should be further investigated.

As mentioned, the PML NBs were manually counted and visual inspection was used to analyze the PML body number in each daughter cell. It is important to interpret such subjective analysis with caution to avoid biased data. Another factor that needs to be considered is that the sectioning of the skin samples was placed at random positions on the embryo. Flow cytometry and cell sorting could be alternative experimental methods to assess the count of PML bodies in daughter cells. Flow cytometry is a popular method in laboratory diagnostics and is frequently used as a method for quantification of different cell types. However, this methodology would also have some limitations in this experimental setup. First, it would not be possible to distinguish between the daughter cells, meaning that the total value of PML NBs per mitotic cell would be quantified. This would therefore not give information about symmetric or asymmetric distribution of PML bodies in daughter cells. Second limitation for use of flow cytometry is that it can only be performed on cell suspensions, which would limit the comparison of *in vivo* vs. *in vitro* studies. Therefore, IHC and manual inspection of samples currently appear as the most optimal method for evaluation of the distribution of PML bodies in mitotic cells.

5.2 Orientation of the cell division in mitotic basal cells in mice epidermis

During the lifespan of an organism, cell division occurs during development, homeostasis and wound healing. During cell cycle, the cell content becomes duplicated and subsequently divided into two daughter cells (Alberts et al. 2015; Schafer 1998). As mentioned, cell divisions are

important in epidermis to maintain and protect the surface of the body, and the cell division can have a horizontal or vertical orientation in the basal layer (Fuchs 2008). While horizontal cell divisions generally produces two identical daughter cells, a vertical mitosis leads to asymmetric cell division and cell differentiation. Thus, the mechanisms controlling the balance between horizontal and vertical orientation is critical for epidermal development and regeneration. In the present theses, we wanted to investigate if PML play a role in mitosis orientation in epidermis.

PMLs role in orientation of cell division was investigated by measuring the angle of mitotic basal cells in relation to the basement membrane (Figure 12). PML wildtype cells at E15.5 had approximately equal fractions of cell division horizontally (~38%) and oblique (~38%), while ~25% of cells had perpendicular orientation. At this stage of embryogenesis, the basal layer expands and formation of the suprabasal cell layers have just started (Williams et al. 2014). Therefore, the fraction of horizontal and oblique divisions are expected to dominate. These data are similar to results obtained by Williams et al. (2014), where a tendency of a higher fraction of horizontal and oblique cell divisions was observed. At E17.5, the same study showed that basal cells had about equal amount of horizontal versus vertical orientation of the cell divisions (Williams et al. 2014). In the present thesis, the tendency was similar as ~34% of the cell divisions were found to have a planer cell division axis while perpendicular cell divisions consisted of ~39% at day 17.5 of embryonic development. The oblique cell divisions were reduced to ~26%. At this embryonic stage, the epidermis is almost fully stratified and maintains the level of basal and suprabasal cells. Statistical analysis did not reveal any significant differences in the orientation of the cell divisions between E15.5 and E17.5 (Table 3).

When comparing the angles of cell division between PML wildtype and PML depleted mice epidermis in Figure 12, the rose diagrams indicate that there might be a difference as the cells with no PML expression seems to have a more randomized distribution of division angles compared to the PML wildtype cells. This was especially noticeable at E17.5 where the PML depleted cells were observed to have approximately equal distribution of horizontal (~31%), oblique (~31%) and vertical (~38%) cell divisions. However, statistical analyses did not reveal any significant difference between PML wildtype and PML depleted mice. A larger sample number is needed in order to verify if the absence of PML leads to a more stochastic division axis distribution. Possible consequences of random cell division orientation of the basal cells are not known. Phenotypic defects related to epidermal thickness and ratios between basal and

suprabasal cells should be investigated in order to determine if a role of PML in division angle regulation is important for normal skin development. However, we are not aware of any reported phenotypic differences of the skin between wildtype and PML depleted mice at birth.

5.3 Aggregation of PML in mitotic MEKs

In human cells, the nuclear PML bodies have been shown to aggregate into larger clusters consisting of multiple monomeric structures called MAPPs following entry into mitosis. At the same time, the number of PML NBs dropped concomitant with de-sumoylation and the loss of Daxx, SP100 and SUMO (Dellaire et al. 2006a; Dellaire et al. 2006b). Aggregation of PML bodies in cells of mice origin, have not previously been reported. A possible consequence of PML body aggregating during mitosis could be that fewer entities of PML in the form of MAPPs could more easily be asymmetrically distributed. Thus, we hypothesized that the lack of asymmetric PML body distribution during mitosis in mice cells may occur do to a failure of PML bodies to aggregate during cell division. To analyze this, the area of the four largest PML NBs were measured in interphase nucleus and in mitotic cells. The results showed that PML bodies in interphase nucleus are significantly smaller than PML bodies detected in mitosis (Figure 15). To our knowledge, this is the first reported aggregation of PML bodies in mitotic cells of mice origin.

5.4 PML and Nup98 co-localizes within CyPNs after treatment with ATO

After mitosis, PML complex with nucleoporins in the cytoplasm and generates CyPNs. These become disassembled and imported into the nucleus during early G_1 in order to re-generate PML NBs (Everett et al. 1999; Jul-Larsen et al. 2009). When cells become treated with ATO, however, the CyPNs become sequestered in the cytoplasm (Zhang et al. 2010). ATO interacts with the PML moiety of the PML/RARA oncoprotein resulting in degradation of PML and PML/RARA by proteasome or autophagosome-dependent degradation pathways (Isakson et al. 2010; Lallemand-Breitenbach et al. 2008). Jul-Larsen et al. (2009) investigated co-localization of PML and cytoplasmic nucleoporines within CyPNs after ATO-treatment in HaCaT and U2OS (human osteosarcoma) cells. They discovered that the co-localization occur during mitosis-to-G_1 transition and that CyPNs moves on the microtubular network until the CyPNs encounter the nuclear membrane. Therefore, CyPNs were also seen to accumulate close to the nuclear membrane. Formation of CyPNs in mouse cells have not previously been reported, and

it is not known if ATO interferes with CyPN sequestration and PML nuclear import in this species.

In this thesis, PML and Nup98 were observed to co-localize within CyPNs after treatment with ATO in mouse cells (Figure 16). MEFs and HDFs were cultured for 4 and 24h hour with or without 0.25µM ATO. The number of cytoplasmic PML bodies were found to decrease with increasing length of ATO-treatment for both cell types, and ATO was observed to stabilize the formation of CyPNs. Although, ATO is found to arrest most of the CyPNs in the cytoplasm (Lång et al. 2012), the cells continue their progression through the cell cycle. In this way, CyPNs can slowly become imported into the nucleus and therefore explain the peak of CyPNs after 4h ATO-treatment. Statistical analyses did not reveal significant changes in all of the compared treatments (Graph 2). A higher amount of investigated cells may provide a more representative result.

5.5 Conclusions

In this thesis, PML bodies were investigated in mitotic basal cells in mice epidermis and in cultured MEKs, MEFs and HDFs. During mitosis, PML bodies were found to become predominantly symmetrically distributed to both daughter cells in embryonic epidermis and in cultured MEKs and MEFs. This differs from a recent unpublished study in human cultured keratinocytes, where PML bodies were observed to have a complete asymmetric distribution in more than 25% of cell divisions (Lång et al. Unpublished 2016). This difference between human and mice keratinocytes suggests that different mechanisms are utilized for the distribution of PML bodies during mitosis. While human cells appear to have evolved mechanisms that allows asymmetric partitioning of PML bodies during mitosis, mouse cells seems to employ mechanisms that promote equal distribution.

The role of PML bodies in the orientation of cell division was further investigated in embryonic PML wildtype and PML depleted mice epidermis. No statistical differences were found between the two embryonic stages or the two genotypes. However, at E15.5 the cell division was mostly planar and oblique while at E17.5 horizontal and planar orientation of the cell divisions dominated. When comparing PML wildtype and PML depleted epidermis, the PML depleted basal cells tends to have a more random orientation of the cell division compared to the PML wildtype. This can possibly alter or delay the development of epidermis before birth,

however, more cells should be analyzed to determine the effects of PML depletion on orientation of cell division in basal cells in tissue.

During mitosis of MEKs, PML bodies were found to aggregate into larger PML bodies. This result is in consistent with previous studies in human cells showing that PML bodies aggregates upon entry into mitosis. To our knowledge, this is the first report of PML aggregation during mitosis in cells from mice. PML bodies were also found to co-localize with nucleoporins into CyPNs after treatment with ATO in MEFs and HDFs. As the length of ATO-treatment increased, the number of PML bodies decreased concomitant with stabilization of PML within the CyPNs. Thus, PML bodies seem to behave similar in mouse and human cells with respect to mitotic aggregation and ATO induced CyPN stabilization. This result shows that the mechanisms regulating the behavior of PML bodies during cell division is conserved from mouse to human.

In summary, PML bodies can be detected in vast majority of cell types and participate in several cellular processes, including basal cells in mice epidermis. That PML bodies becomes symmetrically distributed between daughter cells in mice epidermis is an interesting difference to human cells where complete asymmetric distribution of PML bodies during cell division is quite frequent. This knowledge can be valuable in further research aimed at investigating mechanisms involved in asymmetric partitioning of nuclear components during mitotic cell division.

5.6 Future perspectives

The presence of high levels of PML bodies in basal epidermal cells suggests that PML and PML bodies might have a role in epidermal cell division and/or differentiation. Quantification of PML bodies in daughter cells could be performed by comparing the number of these structures in basal and suprabasal daughter cells instead of dividing into PML rich and PML poor. If a low ratio of PML body asymmetry were detected, it would be interesting to determine if the basal daughter cell is more likely to inherit the largest amount of PML bodies as opposed to the suprabasal daughter. If basal and suprabasal daughters inherit the same number of PML bodies, this would support a symmetric segregation model in mice.

How the mechanism differs in distributing PML bodies in mice and human keratinocytes would be interesting to understand. As PML bodies were found to accumulate to one side of the nucleus in early mitosis during asymmetric segregation in human keratinocytes, it would be interesting to investigate if this also is the case in mice. A possible experimental approach is live cell imagination of MEKs where the progression of PML bodies through mitosis can be directly visualized by time-lapse imaging. A possible result from such experiment can be that the PML bodies only accumulates to one side in cells of human origin and not in cells from mice. If so, this would indicate that human cells, but not mouse cells, possess a mechanism to actively distribute proteins to one side during entry into mitosis. On the other side, if this accumulation is found to occur in both human and mice cells, other mechanisms may therefore exist in mice to symmetrically distribute the PML bodies between daughter cells.

PML bodies might have a role in the orientation of the cell division of basal cells in mice epidermis as shown in this study, although more cells should be analyzed to validate this. In addition, development of the different layers of epidermis should be analyzed when comparing PML wildtype and PML depleted mice embryos. A delayed or altered development of epidermis in PML depleted embryos could indicate that presence of PML is acquired for normal development of skin. It would be interesting to investigate these mechanisms further as they may be relevant for better understanding of epidermal wound healing and cancer.

6 References

Abbas, T. & Dutta, A. (2009). p21 in cancer: intricate networks and multiple activities. *Nature Reviews Cancer*, 9 (6): 400-414.

Abcam. (2013/2014). *Abcam Protocols book*. http://docs.abcam.com/pdf/misc/abcam-protocols-book-2010.pdf (accessed: 15.06.2015).

Alberts, B., Johnson, A., Lewis, J., Morgan, D., Raff, M., Roberts, K. & Walter, P. (2015). Molecular Biology of the Cell. In, pp. 573-1147. New York: Garland Science.

Bernardi, R. & Pandolfi, P. P. (2007). Structure, dynamics and functions of promyelocytic leukaemia nuclear bodies. *Nature reviews Molecular cell biology*, 8 (12): 1006-1016.

Betschinger, J., Mechtler, K. & Knoblich, J. A. (2003). The Par complex directs asymmetric cell division by phosphorylating the cytoskeletal protein Lgl. *Nature*, 422 (6929): 326-330.

Betschinger, J. & Knoblich, J. A. (2004). Dare to be different: asymmetric cell division in Drosophila, C. elegans and vertebrates. *Current biology*, 14 (16): R674-R685.

Blanpain, C. & Fuchs, E. (2006). Epidermal stem cells of the skin. *Annual review of cell and developmental biology*, 22: 339.

Blanpain, C. & Fuchs, E. (2009). Epidermal homeostasis: a balancing act of stem cells in the skin. *Nature reviews Molecular cell biology*, 10 (3): 207-217.

Borden, K. L. (2002). Pondering the promyelocytic leukemia protein (PML) puzzle: possible functions for PML nuclear bodies. *Molecular and cellular biology*, 22 (15): 5259-5269.

Bowman, S. K., Neumüller, R. A., Novatchkova, M., Du, Q. & Knoblich, J. A. (2006). The Drosophila NuMA Homolog Mud regulates spindle orientation in asymmetric cell division. *Developmental cell*, 10 (6): 731-742.

Bragulla, H. H. & Homberger, D. G. (2009). Structure and functions of keratin proteins in simple, stratified, keratinized and cornified epithelia. *Journal of anatomy*, 214 (4): 516-559.

Braissant, O., Foufelle, F., Scotto, C., Dauça, M. & Wahli, W. (1996). Differential expression of peroxisome proliferator-activated receptors (PPARs): tissue distribution of PPAR-alpha,-beta, and-gamma in the adult rat. *Endocrinology*, 137 (1): 354-366.

Butler, K., Martinez, L. & Tejada-Simon, M. (2013). Impaired cognitive function and reduced anxiety-related behavior in a promyelocytic leukemia (PML) tumor suppressor protein-deficient mouse. *Genes, Brain and Behavior*, 12 (2): 189-202.

Bøe, S. O., Haave, M., Jul-Larsen, Å., Grudic, A., Bjerkvig, R. & Lønning, P. E. (2006). Promyelocytic leukemia nuclear bodies are predetermined processing sites for damaged DNA. *Journal of cell science*, 119 (16): 3284-3295.

Candi, E., Schmidt, R. & Melino, G. (2005). The cornified envelope: a model of cell death in the skin. *Nature reviews Molecular cell biology*, 6 (4): 328-340.

Candi, E., Rufini, A., Terrinoni, A., Dinsdale, D., Ranalli, M., Paradisi, A., De Laurenzi, V., Spagnoli, L., Catani, M. & Ramadan, S. (2006). Differential roles of p63 isoforms in epidermal development: selective genetic complementation in p63 null mice. *Cell Death & Differentiation*, 13 (6): 1037-1047.

CellnTec. *General Cultivation Protocol*. http://cellntec.com/wp-content/uploads/pdf/General_Cultivation.pdf (accessed: 14.01.2016).

CellnTec. *Mouse Keratinocyte Isolation*. http://cellntec.com/wp-content/uploads/pdf/Isolation_Keratinocyte_mouse.pdf (accessed: 06.01.2016).

Chen, Y.-C. M., Kappel, C., Beaudouin, J., Eils, R. & Spector, D. L. (2008). Live cell dynamics of promyelocytic leukemia nuclear bodies upon entry into and exit from mitosis. *Molecular biology of the cell*, 19 (7): 3147-3162.

Chen, Z.-X., Xue, Y.-Q., Zhang, R., Tao, R.-F., Xia, X.-M., Li, C., Wang, W., Zu, W.-Y., Yao, X.-Z. & Ling, B.-J. (1991). A clinical and experimental study on all-trans retinoic acid-treated acute promyelocytic leukemia patients. *Blood*, 78 (6): 1413-1419.

Cokol, M., Nair, R. & Rost, B. (2000). Finding nuclear localization signals. *EMBO reports*, 1 (5): 411-415.

Cuchet, D., Sykes, A., Nicolas, A., Orr, A., Murray, J., Sirma, H., Heeren, J., Bartelt, A. & Everett, R. D. (2011). PML isoforms I and II participate in PML-dependent restriction of HSV-1 replication. *Journal of cell science*, 124 (2): 280-291.

Dellaire, G. & Bazett-Jones, D. P. (2004). PML nuclear bodies: dynamic sensors of DNA damage and cellular stress. *Bioessays*, 26 (9): 963-977.

Dellaire, G., Ching, R. W., Dehghani, H., Ren, Y. & Bazett-Jones, D. P. (2006a). The number of PML nuclear bodies increases in early S phase by a fission mechanism. *Journal of cell science*, 119 (6): 1026-1033.

Dellaire, G., Eskiw, C. H., Dehghani, H., Ching, R. W. & Bazett-Jones, D. P. (2006b). Mitotic accumulations of PML protein contribute to the re-establishment of PML nuclear bodies in G1. *Journal of cell science*, 119 (6): 1034-1042.

Derivery, E., Seum, C., Daeden, A., Loubéry, S., Holtzer, L., Jülicher, F. & Gonzalez-Gaitan, M. (2015). Polarized endosome dynamics by spindle asymmetry during asymmetric cell division. *Nature*, 528 (7581): 280-285.

Devenport, D., Oristian, D., Heller, E. & Fuchs, E. (2011). Mitotic internalization of planar cell polarity proteins preserves tissue polarity. *Nature cell biology*, 13 (8): 893-902.

Dewey, E. B., Taylor, D. T. & Johnston, C. A. (2015). Cell Fate Decision Making through Oriented Cell Division. *Journal of Developmental Biology*, 3 (4): 129-157.

Doe, C. Q. (1992). Molecular markers for identified neuroblasts and ganglion mother cells in the Drosophila central nervous system. *Development*, 116 (4): 855-863.

Doe, C. Q. (1996). Asymmetric cell division and neurogenesis. *Current opinion in genetics & development*, 6 (5): 562-566.

Eskiw, C. H., Dellaire, G. & Bazett-Jones, D. P. (2004). Chromatin contributes to structural integrity of promyelocytic leukemia bodies through a SUMO-1-independent mechanism. *Journal of Biological Chemistry*, 279 (10): 9577-9585.

Estey, E., Garcia-Manero, G., Ferrajoli, A., Faderl, S., Verstovsek, S., Jones, D. & Kantarjian, H. (2006). Use of all-trans retinoic acid plus arsenic trioxide as an alternative to chemotherapy in untreated acute promyelocytic leukemia. *Blood*, 107 (9): 3469-3473.

Everett, R. D., Lomonte, P., Sternsdorf, T., van Driel, R. & Orr, A. (1999). Cell cycle regulation of PML modification and ND10 composition. *Journal of Cell Science*, 112 (24): 4581-4588.

Forni, M. F., Trombetta-Lima, M. & Sogayar, M. C. (2012). Stem cells in embryonic skin development. *Biological research*, 45 (3): 215-222.

Frick, A., Suzuki, O., Butz, N., Chan, E. & Wiltshire, T. (2013). In Vitro and In Vivo Mouse Models for Pharmacogenetic Studies In Innocenti, F. & Schaik, R. H. N. v. (eds) *Pharmacogenomics Methods and Protocols* pp. 263-265. New York: Humana Press.

Fuchs, E. (1995). Keratins and the skin. *Annual review of cell and developmental biology*, 11 (1): 123-154.

Fuchs, E., Tumbar, T. & Guasch, G. (2004). Socializing with the neighbors: stem cells and their niche. *Cell*, 116 (6): 769-778.

Fuchs, E. (2008). Skin stem cells: rising to the surface. *The Journal of cell biology*, 180 (2): 273-284.

Gaglio, T., Saredi, A. & Compton, D. A. (1995). NuMA is required for the organization of microtubules into aster-like mitotic arrays. *The Journal of Cell Biology*, 131 (3): 693-708.

Goldstein, B. & Macara, I. G. (2007). The PAR proteins: fundamental players in animal cell polarization. *Developmental cell*, 13 (5): 609-622.
Grignani, F., Ferrucci, P. F., Testa, U., Talamo, G., Fagioli, M., Alcalay, M., Mencarelli, A., Grignani, F., Peschle, C. & Nicoletti, I. (1993). The acute promyelocytic leukemia-specific PML-RARα fusion protein inhibits differentiation and promotes survival of myeloid precursor cells. *Cell*, 74 (3): 423-431.
Hawkins, N. & Garriga, G. (1998). Asymmetric cell division: from A to Z. *Genes & development*, 12 (23): 3625-3638.
Horvitz, H. R. & Herskowitz, I. (1992). Mechanisms of asymmetric cell division: two Bs or not two Bs, that is the question. *Cell*, 68 (2): 237-255.
Hsu, Y.-C., Li, L. & Fuchs, E. (2014). Emerging interactions between skin stem cells and their niches. *Nature medicine*, 20 (8): 847-856.
Inc., Y. T. (2016). *Online Rose Diagram*. http://www.yongtechnology.com/yong-lab/online-rose-diagram/ (accessed: 12.01.2016).
Ing, V. W. (1984). The Etiology and Management of Leukopenia. *Canadian Family Physician*, 30: 1835.
Isakson, P., Bjørås, M., Bøe, S. O. & Simonsen, A. (2010). Autophagy contributes to therapy-induced degradation of the PML/RARA oncoprotein. *Blood*, 116 (13): 2324-2331.
Ishov, A. M., Sotnikov, A. G., Negorev, D., Vladimirova, O. V., Neff, N., Kamitani, T., Yeh, E. T., Strauss, J. F. & Maul, G. G. (1999). PML is critical for ND10 formation and recruits the PML-interacting protein daxx to this nuclear structure when modified by SUMO-1. *The Journal of cell biology*, 147 (2): 221-234.
Ito, K., Carracedo, A., Weiss, D., Arai, F., Ala, U., Avigan, D. E., Schafer, Z. T., Evans, R. M., Suda, T. & Lee, C.-H. (2012). A PML-PPAR-[delta] pathway for fatty acid oxidation regulates hematopoietic stem cell maintenance. *Nature medicine*, 18 (9): 1350-1358.
Itoh, F., Divecha, N., Brocks, L., Oomen, L., Janssen, H., Calafat, J., Itoh, S. & Dijke, P. t. (2002). The FYVE domain in Smad anchor for receptor activation (SARA) is sufficient for localization of SARA in early endosomes and regulates TGF-β/Smad signalling. *Genes to Cells*, 7 (3): 321-331.
Jan, Y. N. & Jan, L. Y. (1998). Asymmetric cell division. *Nature*, 392 (6678): 775-778.
Jensen, K., Shiels, C. & Freemont, P. S. (2001). PML protein isoforms and the RBCC/TRIM motif. *Oncogene*, 20 (49): 7223-7233.
Jones, M. E. & Saleem, A. (1978). Acute promyelocytic leukemia: A review of literature. *The American journal of medicine*, 65 (4): 673-677.
Jul-Larsen, Å., Visted, T., Karlsen, B. O., Rinaldo, C. H., Bjerkvig, R., Lønning, P. E. & Bøe, S. O. (2004). PML-nuclear bodies accumulate DNA in response to polyomavirus BK and simian virus 40 replication. *Experimental cell research*, 298 (1): 58-73.
Jul-Larsen, Å., Grudic, A., Bjerkvig, R. & Bøe, S. O. (2009). Cell-cycle regulation and dynamics of cytoplasmic compartments containing the promyelocytic leukemia protein and nucleoporins. *Journal of cell science*, 122 (8): 1201-1210.
King, K. & Cidlowski, J. (1998). Cell cycle regulation and apoptosis 1. *Annual review of physiology*, 60 (1): 601-617.
Knoblich, J. A. (2008). Mechanisms of asymmetric stem cell division. *Cell*, 132 (4): 583-597.
Koken, M., Reid, A., Quignon, F., Chelbi-Alix, M., Davies, J., Kabarowski, J., Zhu, J., Dong, S., Chen, S.-J. & Chen, Z. (1997). Leukemia-associated retinoic acid receptor α fusion partners, PML and PLZF, heterodimerize and colocalize to nuclear bodies. *Proceedings of the National Academy of Sciences*, 94 (19): 10255-10260.
Koster, M. I. & Roop, D. R. (2007). Mechanisms regulating epithelial stratification. *Annu. Rev. Cell Dev. Biol.*, 23: 93-113.

Kulukian, A. & Fuchs, E. (2013). Spindle orientation and epidermal morphogenesis. *Philosophical Transactions of the Royal Society of London B: Biological Sciences*, 368 (1629): 20130016.

Lallemand-Breitenbach, V., Jeanne, M., Benhenda, S., Nasr, R., Lei, M., Peres, L., Zhou, J., Zhu, J., Raught, B. & de Thé, H. (2008). Arsenic degrades PML or PML–RARα through a SUMO-triggered RNF4/ubiquitin-mediated pathway. *Nature cell biology*, 10 (5): 547-555.

Lallemand-Breitenbach, V. (2010). PML nuclear bodies. *Cold Spring Harbor perspectives in biology*, 2 (5): a000661.

Lanottei, M., Degos, L. & Deiean, A. (1990). The t (15; 17) translocation of acute promyelocytic leukaemia fuses the retinoic acid receptor or gene to a novel transcribed locus. *Nature*, 347.

Lechler, T. & Fuchs, E. (2005). Asymmetric cell divisions promote stratification and differentiation of mammalian skin. *Nature*, 437 (7056): 275-280.

Li, J., Gu, L., Zhang, H., Liu, T., Tian, D., Zhou, M. & Zhou, S. (2013). Berberine represses DAXX gene transcription and induces cancer cell apoptosis. *Laboratory Investigation*, 93 (3): 354-364.

Li, W., Ferguson, B. J., Khaled, W. T., Tevendale, M., Stingl, J., Poli, V., Rich, T., Salomoni, P. & Watson, C. J. (2009). PML depletion disrupts normal mammary gland development and skews the composition of the mammary luminal cell progenitor pool. *Proceedings of the National Academy of Sciences*, 106 (12): 4725-4730.

Lichti, U., Anders, J. & Yuspa, S. H. (2008). Isolation and short-term culture of primary keratinocytes, hair follicle populations and dermal cells from newborn mice and keratinocytes from adult mice for in vitro analysis and for grafting to immunodeficient mice. *Nature protocols*, 3 (5): 799-810.

Liu, S., Zhang, H. & Duan, E. (2013). Epidermal development in mammals: key regulators, signals from beneath, and stem cells. *International journal of molecular sciences*, 14 (6): 10869-10895.

Lunardi, A., Gaboli, M., Giorgio, M., Rivi, R., Bygrave, A., Antoniou, M., Drabek, D., Dzierzak, E., Fagioli, M. & Salmena, L. (2011). A role for PML in innate immunity. *Genes & cancer*, 2 (1): 10-19.

Lång, E. & Bøe, S. O. (2011). Acute Promeyelocytic Leukemia: A Model Disease for Targeted Cancer Therapy. In Koschmieder, S. & Krug, U. (eds) *Myeloid leukemia Basic mechanisms of leukemogenesis* pp. 363-384. Croatia: InTech.

Lång, E., Grudic, A., Pankiv, S., Bruserud, Ø., Simonsen, A., Bjerkvig, R., Bjørås, M. & Bøe, S. O. (2012). The arsenic-based cure of acute promyelocytic leukemia promotes cytoplasmic sequestration of PML and PML/RARA through inhibition of PML body recycling. *Blood*, 120 (4): 847-857.

Lång, E., Połeć, A., Lång, A., Blicher, P., Rowe, A. D., Jackson, C., Utheim, T. P., Eriksson, J. & Bøe, S. O. (Unpublished 2016). Coordinated Collective Migration and Oriented Nuclear Partitioning in Sheets of Cultured Human Keratinocytes.

Miller, S. W., Avidor-Reiss, T., Polyanovsky, A. & Posakony, J. W. (2009). Complex interplay of three transcription factors in controlling the tormogen differentiation program of Drosophila mechanoreceptors. *Developmental biology*, 329 (2): 386-399.

Ming, G.-l. & Song, H. (2011). Adult neurogenesis in the mammalian brain: significant answers and significant questions. *Neuron*, 70 (4): 687-702.

Nasr, R., Guillemin, M.-C., Ferhi, O., Soilihi, H., Peres, L., Berthier, C., Rousselot, P., Robledo-Sarmiento, M., Lallemand-Breitenbach, V. & Gourmel, B. (2008). Eradication of acute promyelocytic leukemia-initiating cells through PML-RARA degradation. *Nature medicine*, 14 (12): 1333-1342.

Newhart, A., Negorev, D. G., Rafalska-Metcalf, I. U., Yang, T., Maul, G. G. & Janicki, S. M. (2013). Sp100A promotes chromatin decondensation at a cytomegalovirus-promoter–regulated transcription site. *Molecular biology of the cell*, 24 (9): 1454-1468.

Palibrk, V., Lång, E., Lång, A., Schink, K. O., Rowe, A. D. & Bøe, S. O. (2014). Promyelocytic leukemia bodies tether to early endosomes during mitosis. *Cell Cycle*, 13 (11): 1749-1755.

Piazza, F., Gurrieri, C. & Pandolfi, P. P. (2001). The theory of APL. *Oncogene*, 20 (49): 7216-7222.

Pines, J. & Rieder, C. L. (2001). Re-staging mitosis: a contemporary view of mitotic progression. *Nature cell biology*, 3 (1): E3-E6.

Puccetti, E. & Ruthardt, M. (2004). Acute promyelocytic leukemia: PML/RARα and the leukemic stem cell. *Leukemia*, 18 (7): 1169-1175.

Regad, T., Bellodi, C., Nicotera, P. & Salomoni, P. (2009). The tumor suppressor Pml regulates cell fate in the developing neocortex. *Nature neuroscience*, 12 (2): 132-140.

Reymond, A., Meroni, G., Fantozzi, A., Merla, G., Cairo, S., Luzi, L., Riganelli, D., Zanaria, E., Messali, S. & Cainarca, S. (2001). The tripartite motif family identifies cell compartments. *The EMBO journal*, 20 (9): 2140-2151.

Rhyu, M. S., Jan, L. Y. & Jan, Y. N. (1994). Asymmetric distribution of numb protein during division of the sensory organ precursor cell confers distinct fates to daughter cells. *Cell*, 76 (3): 477-491.

Salomoni, P., Ferguson, B. J., Wyllie, A. & Rich, T. (2008). New insights into the role of PML in tumour suppression. *Cell research*, 18 (6): 622-640.

Sancar, A., Lindsey-Boltz, L. A., Ünsal-Kaçmaz, K. & Linn, S. (2004). Molecular mechanisms of mammalian DNA repair and the DNA damage checkpoints. *Annual review of biochemistry*, 73 (1): 39-85.

Schafer, K. (1998). The cell cycle: a review. *Veterinary Pathology Online*, 35 (6): 461-478.

Selbach, M., Schwanhäusser, B., Thierfelder, N., Fang, Z., Khanin, R. & Rajewsky, N. (2008). Widespread changes in protein synthesis induced by microRNAs. *nature*, 455 (7209): 58-63.

Shen, C.-P., Jan, L. Y. & Jan, Y. N. (1997). Miranda is required for the asymmetric localization of Prospero during mitosis in Drosophila. *Cell*, 90 (3): 449-458.

Shen, T. H., Lin, H.-K., Scaglioni, P. P., Yung, T. M. & Pandolfi, P. P. (2006). The mechanisms of PML-nuclear body formation. *Molecular cell*, 24 (3): 331-339.

Shen, Z.-X., Chen, G.-Q., Ni, J.-H., Li, X.-S., Xiong, S.-M., Qiu, Q.-Y., Zhu, J., Tang, W., Sun, G.-L. & Yang, K.-Q. (1997). Use of arsenic trioxide (As2O3) in the treatment of acute promyelocytic leukemia (APL): II. Clinical efficacy and pharmacokinetics in relapsed patients. *Blood*, 89 (9): 3354-3360.

Shen, Z.-X., Shi, Z.-Z., Fang, J., Gu, B.-W., Li, J.-M., Zhu, Y.-M., Shi, J.-Y., Zheng, P.-Z., Yan, H. & Liu, Y.-F. (2004). All-trans retinoic acid/As2O3 combination yields a high quality remission and survival in newly diagnosed acute promyelocytic leukemia. *Proceedings of the National Academy of Sciences of the United States of America*, 101 (15): 5328-5335.

Shenoy, A. & Blelloch, R. H. (2014). Regulation of microRNA function in somatic stem cell proliferation and differentiation. *Nature Reviews Molecular Cell Biology*, 15 (9): 565-576.

Siller, K. H., Cabernard, C. & Doe, C. Q. (2006). The NuMA-related Mud protein binds Pins and regulates spindle orientation in Drosophila neuroblasts. *Nature Cell Biology*, 8 (6): 594-600.

Siller, K. H. & Doe, C. Q. (2009). Spindle orientation during asymmetric cell division. *Nature cell biology*, 11 (4): 365-374.

Song, J., Durrin, L. K., Wilkinson, T. A., Krontiris, T. G. & Chen, Y. (2004). Identification of a SUMO-binding motif that recognizes SUMO-modified proteins. *Proceedings of the National Academy of Sciences of the United States of America*, 101 (40): 14373-14378.

Stone, R. M. & Mayer, R. (1990). The unique aspects of acute promyelocytic leukemia. *Journal of Clinical Oncology*, 8 (11): 1913-1921.

Thavarajah, R., Mudimbaimannar, V. K., Elizabeth, J., Rao, U. K. & Ranganathan, K. (2012). Chemical and physical basics of routine formaldehyde fixation. *Journal of Oral and Maxillofacial Pathology*, 16 (3): 400.

ThermoFisher. (2009). *Human Dermal Fibroblasts, adult (HDFa)*. https://tools.thermofisher.com/content/sfs/manuals/HDFa_man.pdf (accessed: 01.12.2015).

Wang, H., Somers, G. W., Bashirullah, A., Heberlein, U., Yu, F. & Chia, W. (2006). Aurora-A acts as a tumor suppressor and regulates self-renewal of Drosophila neuroblasts. *Genes & development*, 20 (24): 3453-3463.

Wang, Z.-G., Ruggero, D., Ronchetti, S., Zhong, S., Gaboli, M., Rivi, R. & Pandolfi, P. P. (1998). PML is essential for multiple apoptotic pathways. *Nature genetics*, 20 (3): 266-272.

Wang, Z.-Y. & Chen, Z. (2008). Acute promyelocytic leukemia: from highly fatal to highly curable. *Blood*, 111 (5): 2505-2515.

Wang, Z. G., Delva, L., Gaboli, M., Rivi, R., Giorgio, M., Cordon-Cardo, C., Grosveld, F. & Pandolfi, P. P. (1998). Role of PML in cell growth and the retinoic acid pathway. *Science*, 279 (5356): 1547-1551.

Williams, S. E., Ratliff, L. A., Postiglione, M. P., Knoblich, J. A. & Fuchs, E. (2014). Par3–mInsc and Gαi3 cooperate to promote oriented epidermal cell divisions through LGN. *Nature cell biology*, 16 (8): 758-769.

Zhang, X.-W., Yan, X.-J., Zhou, Z.-R., Yang, F.-F., Wu, Z.-Y., Sun, H.-B., Liang, W.-X., Song, A.-X., Lallemand-Breitenbach, V. & Jeanne, M. (2010). Arsenic trioxide controls the fate of the PML-RARα oncoprotein by directly binding PML. *Science*, 328 (5975): 240-243.

Zhong, S., Müller, S., Ronchetti, S., Freemont, P. S., Dejean, A. & Pandolfi, P. P. (2000a). Role of SUMO-1–modified PML in nuclear body formation. *Blood*, 95 (9): 2748-2752.

Zhong, S., Salomoni, P. & Pandolfi, P. P. (2000b). The transcriptional role of PML and the nuclear body. *Nature cell biology*, 2 (5): E85-E90.

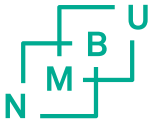

Norges miljø- og biovitenskapelig universitet
Noregs miljø- og biovitskapelege universitet
Norwegian University of Life Sciences

Postboks 5003
NO-1432 Ås
Norway